ADDIS ABABA UNIVERSITY

SCHOOL OF GRADUATE STUDIES

INSTITUTE OF TECHNOLOGY

SCHOOL OF MECHANICAL AND INDUSTRIAL ENGINEERING

IDENTIFYING THE STRESS OF RAIL JOINT UNDER WHEEL LOAD BY CHANGING THE BOLT GEOMETRY

A Thesis Submitted to the School of Graduate Studies of Addis Ababa University in Partial Fulfilment of the Requirements for the Degree of Masters of Science in Mechanical Engineering (Railway stream)

BY

Awet Desta

Advisor

Dr. Daniel Tilahun

May, 2015

ADDIS ABABA UNIVERSITY

SCHOOL OF GRADUATE STUDIES

INSTITUTE OF TECHNOLOGY

SCHOOL OF MECHANICAL AND INDUSTRIAL ENGINEERING

IDENTIFYING THE STRESS OF RAIL JOINT UNDER WHEEL LOAD BY CHANGING THE BOLT GEOMETRY

BY

Awet Desta

Advisor

Dr. Daniel Tilahun

May, 2015

Approved by board of examining:

Dr. Birhanu Beshal	_____	_____
Head, railway center	Signature	Date
Dr. Daniel Tilahun	_____	_____
Advisor	Signature	Date
Mr. Yidnekachew Messele (MSc)	_____	_____
Internal Examiner	Signature	Date
Mr. Tsegaye Feleke (MSc)	_____	_____
External Examiner	Signature	Date

DECLARATION

I, the undersigned, declare that this thesis is my original work and has not been presented for a degree in this or any other universities, and all sources of materials used for the thesis work have been fully acknowledged.

Awet Desta _____ _____

Name Signature Date

This thesis has been submitted for examination with my approval as a university advisor.

Dr. Daniel Tilahun _____ _____

Name Signature Date

Acknowledgments

First of all, I would like to thank God who gave me patience and strength to finish this research. Without his support nothing is possible. I would also like to express my sincere appreciation and gratitude to my advisor Dr.Daniel Tilahun for his support and guidance. I want to appreciate also his willingness and giving of motivations to work on this research.

Thanks also to all workers of Ethiopian Railway Corporation of Addis Ababa Light Rail Transit (LRT) who helped me by giving the necessary materials for the research.

I would like to thank my mother and my sisters Futsum Desta and Makda Desta for encouraging me in all my work. They have supported me very much. I would also like to thank my family and friends, for their support and motivation.

Abstract

It is well known that the fatigue failure of bolts can affect the performance of rail joint and the safety of train running. In this work, the influences of the bolt geometry and bolt material on the stress of the rail joint are studied by Finite Element method. A three -dimensional finite element model for rail joint is developed and wheel load is applied to identify the stress of the rail joint. Different components of the rail joint bolts are being created separately and assemble in CATIA. The model consists of assembly of the rail, joint bars, bolts, nuts, washers, and wheel. A three -dimensional finite element analysis of rail joint bars is carried out in ANSYS after importing from CATIA. The wheel load and velocity are being applied to identify the stress in the rail joint. The material properties of the rail and wheel are assumed to be same. The material properties of the wheel and rail are considered to be bilinear kinematic hardening in ANSYS. All the material properties and boundary conditions are being applied strictly as per the data available by the Ethiopian railway corporation The results indicate that increasing the radius of rounded root rail bolt can reduce the stress concentration at the root of rail bolt and rail joint this will improves the fatigue strength and the working life of the rail bolt and rail joint. And changing the bolt material has an effect to the stress of the bolt.

Contents

List of figures

List of tables

Nomenclature

RJ	Rail joint
IRJ	Insulated Rail Joint
FEM	Finite Element Method
EFA	Finite Element Analysis
AISI	American iron and steel institute
LRT	Light rail transit
a	Minor semi axes of the contact ellipse
b	Major semi axes of the contact ellipse
F	Vertical load
m & n	Hertz coefficients
Kw	Constants that depend on the material properties of railway wheel
$\mathbf{V_W}$	Poisson's ratio wheel material
$\mathbf{E_W}$	Young's modulus of the railway wheel material
$\mathbf{V_R}$	Poisson's ratio of rail material
$\mathbf{E_R}$	Young's modulus of rail material
$\mathbf{R_1}$	Principal rolling radii of the wheel
$\mathbf{R_2}$	Principal rolling radii of rail
$\mathbf{R_1'}$	Principal transverse radii of curvature of wheel
$\mathbf{R_2'}$	Principal transverse radii of curvature of radii
K	Stiffness matrix of the system
U	Nodal displacement vector
$\mathbf{\Gamma_1}$	Boundary with zero displacement,
$\mathbf{\Gamma_2}$	Boundary where measured displacements are given

$\mathbf{\Gamma_3}$	Boundary with unknown contact forces Fc
$\mathbf{\Gamma_4}$	Boundary where there are known applied forces
$\mathbf{F_a}$	Applied forces
$\mathbf{U_1}$	Displacements on constrained boundary Γ_1
$\mathbf{U_2}$	Known and measured displacements on free boundary Γ_2
$\mathbf{U_3}$	Unknown displacements on contact boundary Γ_3
$\mathbf{U_4}$	Unknown displacements on boundary Γ_4
$\boldsymbol{\sigma}$	Stress vector
D	Elastic stiffness matrix.
$\boldsymbol{\epsilon^{el}}$	Strain that cause stress
$\mathbf{E_x}$	Young's modulus in the x direction
$\mathbf{G_{xy}}$	Shear modulus in the xy plane
$\mathbf{V_{xy}}$	Major Poison's ratio
$\mathbf{v_{yx}}$	Minor poison's
$\boldsymbol{\sigma_x}$	Stress in x direction
$\boldsymbol{\sigma_y}$	Stress in y direction
$\boldsymbol{\sigma_z}$	Stress in z direction
$\boldsymbol{\sigma^f{}_{xc}}$	Normal stress failure in x direction
$\mathbf{\sigma^f{}_{yc}}$	Normal stress failure in y direction
$\mathbf{\sigma^f{}_{zc}}$	Normal stress failure in z direction
$\boldsymbol{\sigma_{xy}}$	Shear failure in xy direction
$\boldsymbol{\sigma_{yz}}$	Shear failure in yz direction
$\boldsymbol{\sigma_{xz}}$	Shear failure in xz direction

Chapter one

1. Introduction

1.1. Background of the study

The track or Permanent Way is the rail-road on which trains run. It basically consists of parallel rails having a specified distance in between and fastened to sleepers, which are embedded in a layer of ballast of specified thickness spread over the formation. The rail are joined each other by fish plates and bolts and these are fastened to the sleepers by various fittings like keys and spikes etc. the sleepers are spaced at a specified distance and are held in position by embedding in ballast. Each of the components of track has a basic function to perform. The rails act as girders to transmit the wheel loads of trains to the sleepers. The sleepers hold the rails in proper position and provide a correct gauge with the help of fitting and fastenings and transfer the load to the ballast is placed on level ground known as formation. The sleepers are embedded in ballast, which gives a uniform level surface, provides drainage and transfers the load to a larger area of formation. The formation gives a level surface, where the ballast rests and takes the total load of the track and that of the trains moving on it.

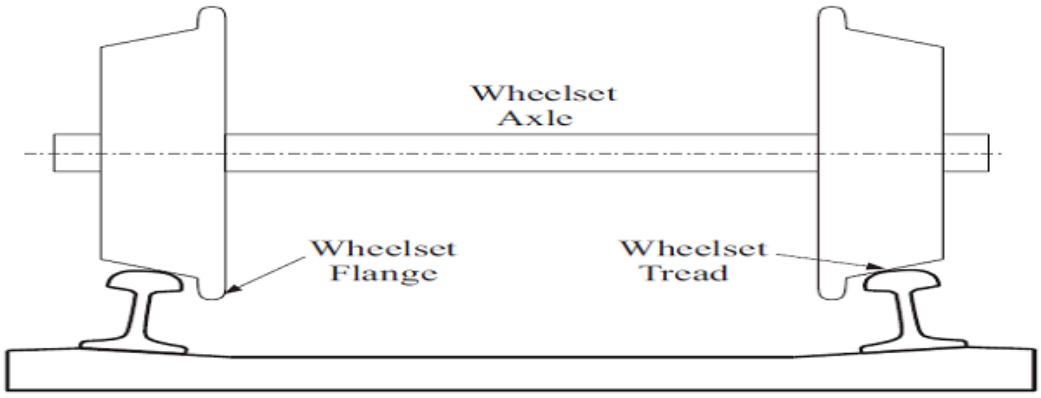

Figure1.1: Assembly of rail wheel axle.

Fig.:1.1 Show assembly of wheel rail contact. Among all the sub-systems and the components that are a part of a railway system, the wheel/rail interface is one of the most delicate, both as regards the performances of the train and as regards its safety. Indeed the problem is complex, due to the fact that damage of the wheel/rail interface depends on many factors and different mechanisms contribute to the deterioration of the contact surfaces. Wear, rolling contact fatigue are the most common types of damage due to the wheel/rail contact. Among all the damage mechanisms, fatigue is one of the most frequent ones. Fatigues causes abrupt fractures in wheel or tread surface material loss. In order to accurately describe

the stress state under contact condition, Hertz in Germany gave a more detailed theory to determine the area of contact and the pressure distribution at the surface of contact between the rail and the wheel. As per this theory, the rail and wheel contact is similar to that of two cylinders (the circular wheel and curved head of the head of the rail) with their axes right angles to each other.

Referring to Fig.1.2, rail joints may be classified as either insulated or bolted joints [6]. Insulated joints may be bonded (in which the joint bars are epoxied to the rail) or non-bonded (which are basically bolted joints with electrical insulating properties). Bolted joints consist of either compromise or standard joints. Compromise bars are used to join two rails of unequal size (e.g. joining 115 lb rail and 140 lb rail). Standard joints may be either temporary or permanent.

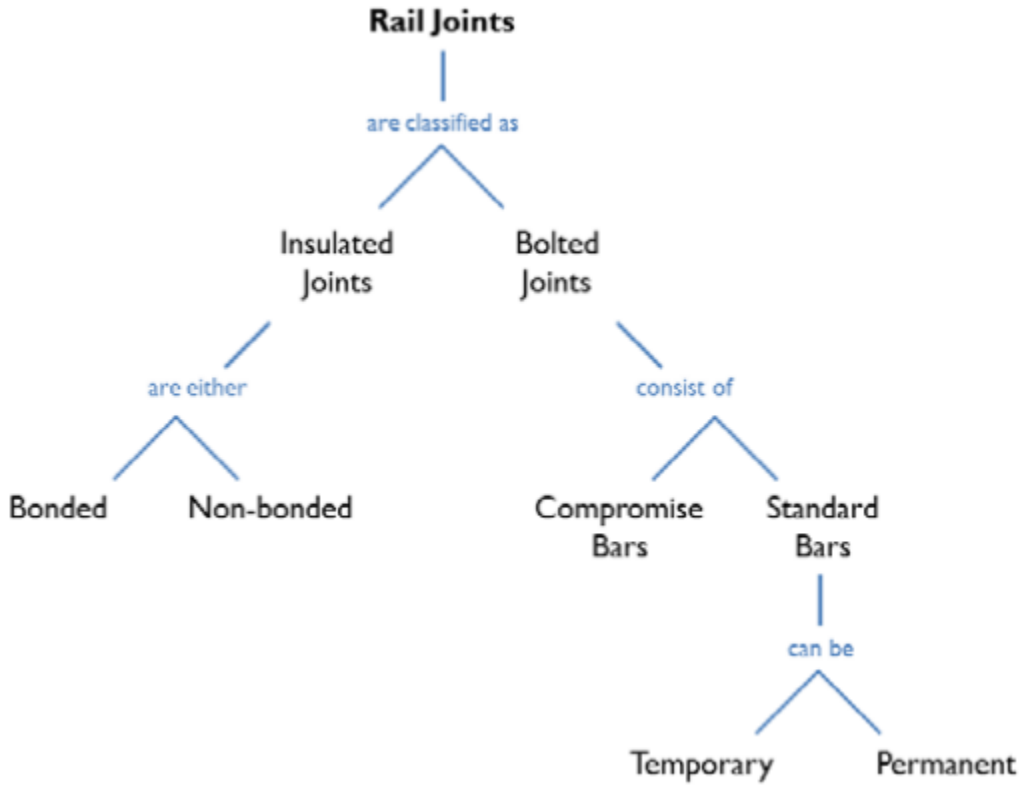

Figure 1.2: Classification of Rail Joints

A rail joint is the weakest spots in the railway track. Rail joint are used to connect the ends of two rails horizontally and vertically. The continuity of the railway track is breaks due to the existence of rail gap and difference in the height of the rail heads. Because of the above reasons rail joints are weaker than the rails and subjected to large stress.

Figure: 1.3 a typical rail joint [15]

Figure 1.4 shows a symmetrically suspended joint in between the sleepers as opposed to the rail joint in figure 1.5 which is an unsymmetrically supported one. In relation to supported joints, a discretely supported joint can be seen on a concrete sleeper (figure 1.6) and on a single timber sleeper (figure 1.7) and on double timber sleeper (figure 1.8). In addition, a continuously supported joint is also described in the literature (figure1.9). In this design, joint bars (fishplates) are reshaped to a new form that can be supported over the sleepers.

Figure 1.4: Symmetrically suspended rail joint [10]

Figure 1.5: Unsymmetrically suspended IRJ

Figure1.6: Discrete concrete sleeper supported joint [11]

In practice, 4-bolt joint bars (figure1.4) and 6-bolt joint bars (figure1.6) are most popular. Because of higher number of bolts, the length of joint bar is also different. As per the Australian Standard [9], lengths of 4-bolt joint bar and 6-bolt joint bar are 576 mm and 830 mm respectively.

Figure1.7: Discreetly supported joint on a timber sleeper

Figure1.8: Supported joint on two timber sleepers [12]

Figure1.9: Continuously supported joints on sleepers [13]

The function of the fishplate is to hold the two rails together both in the horizontal and vertical planes. The fish plates are manufactured from a special type of steel having composition of Carbon, Manganese, Silicon, Sulphur and Phosphorous 0.30 to 0.42%, Not more than 0.8%,

Not more than 0.15%, Not more than 0.06 % respectively. The fish plates are so designed that the fishing angles at the top and bottom surface coincide with those of the rail section so as to have a perfect contact with the rail. Elastic elements (springs) are components which return to their original dimensions when forces causing them to deflect are removed. Elastic elements used to: Equalize the vertical wheels (unloading of any wheel is dangerous because it causes a reduction/loss of guidance forces).Stabilize the motion of vehicles on track (self-excited lateral oscillations i.e., hunting of wheel sets is dangerous).Reduce the dynamic forces and accelerations due to track irregularities.

1.2. Significance of the study

This research has a great impact on future analysis and applications of rail joints in general and in particular in the Ethiopian context. Especially, it will contributes a lot for future analysis of rail joint failures like fatigue, wear . Most practical rail joint installations are seen to be failed out before the specified design periods. This may be due to improper installations and engagements. In addition to that it may be due to improper selection of rail joints and standard geometries. However, this paper provides the general wheel-rail joint models and the bolt geometry to identify the stress in the joint. In this paper the ANSYS software is used to simulate and analysis the wheel/rail joint contact.

1.3. Statement of the problem

The problem of rail bolt hole cracking is not unique to any specific railroad, region or country but is recognized as a world problem. Railroad tracks are continually subjected to high loads generated by the passage of rolling stock. With the need for higher strength to weight ratio of engineering components, fatigue has become a very important phenomenon especially in automobiles, aircrafts which are subject to repeated loading and vibration. Flexing and displacement of rails at bolted joints combine to induce high cyclic tensile and shear loads in the joint bar, or fish plate, which are transferred to the attaching bolt holes.

A rail joint is the weakest link in the track. There is a break in the continuity of the rail in horizontal as well as in vertical plane at this location because of the expansion gap and Imperfection in the rail heads at joint. The fitting at the joint become loose, causing heavy wear and tear to the track materials. It is normally felt that a rail joint requires about 30% extra maintenance than the plain track. so before this kind of damage happens detail researches must be done especially in Ethiopia since our country is introducing this technology. So the main questions that may be raised are:

- What are the main sources of rail joint damage?
- What are the consequences of rail joint damage?
- What types of stresses are inducing on the rail joint due to wheel load?
- How stresses are causing the deflection on rail joint?

1.4. The objectives of the study

1.4.1. General objective

The objective of this thesis is to use finite element analysis to identify the stress in rail joints. First the finite element analysis program ANSYS is tested to verify its ability to correctly model the interaction of the rail and joint. By changing the bolt geometry the stresses in the joint will be identified.

1.4.2. Specific objective

- Gathering information's and data's about the current Ethiopian railway corporation rail joints, wheels, rails, and materials etc…..which are set for LRT.
- Gathering various softwares which are helpful for this study.
- 3-D Modeling of rails, wheels, and joint by using CATIA, and simulating the results by ANSYS software.
- Studying the stresses that exist in joints, and rails.
- Comparing the results of finite element method with that of theoretical formulations.

1.5. Limitations

The aims of this thesis are to identify the stress in joints and rail by changing the bolt geometry and bolt material using ANSYS software. The method is restricted to evaluate fatigue. No economic analysis is carried out in the project, however the results can serve as background for refined such analyses since it facilitates predictions of stress in the joints.

The model does not account for factors such as dynamic effects, the direction of passing vehicles or the acceleration or braking of passing trains. If the joint is located close to a station the train will accelerate or brake in while passing the joint, causing unsymmetrical wear on the joint region. This is however not covered in this project but it might be considered as a follow-up project.

1.6. Organization of the Paper

The body of this study is divided into five main chapters. The first chapter discusses background, objectives and methodology of the study. In addition, the details of the rail joint type and rail joint used for analyze. The second chapter covers the review of some of the journal articles, conference papers and publications which were referred to during the study. Also, in relation and comparison with previous works, what is done in this study will be stated. Model and analysis of stress on rail joint is discussed in the third chapter. Modeling contact at rail joint, stress model using hertzian theory, rail support and wheel rail simulation presented. The results obtained from the analysis of the rail joint and discussions based on these results are included in the fourth chapter. Finally, the fifth chapter cover conclusions drawn based on the results of the analysis, recommendations and future work

Chapter Two

2. Literature Review

2.1. Contact Stresses

Hertz contact theory [1], described in Section 2.3, has been used in stress analysis for bodies in contact, and is often applied to the contact between a wheel and rail. [2] supported the use of the Hertz contact patch in his review of the wheel-rail contact problem, stating that since the "wheels and rails are never perfectly rigid", the initial contact point between the two should spread into a finite area and "it is essential to have quantitative information on the size and shape of the contact patch, and on the distribution of the stresses in its immediate neighborhood."

The ability of the Hertz theory to correctly model the wheel-rail contact near a rail end, such as at an end post, was investigated by [3]. His elastic-plastic model revealed that as the wheel load moves toward a rail end, larger plastic zones with increased von Mises stresses occur in the rail, which could cause deterioration of the rail end. In comparing his elastic-plastic model with Hertz contact theory, he learned that the contact length increases, thus decreasing the peak contact pressure, as the center of the wheel load moves closer to the rail end.

Another aspect of research on wheel-rail contact has focused on the dynamics of the problem. [4] Investigated the wheel-rail contact dynamically using finite element analysis. Their sensitivity studies into the effects of axle load and train speed on dynamic vertical forces, stresses, and strain distributions in the railhead determined that the maximum vertical load due to the dynamic impact of the wheel was approximately 2.6 times the static force. Their work also concluded that increasing the axle load also increased the dynamic load and resulting stresses in the railhead, while increasing the train speed had very little effect on the load and stresses.

[5] Investigated the use of Hertz theory as it pertained to modeling the contact stress near insulated railroad joints. Their work focused on the contact pressure felt by the rail and insulated joint when subjected to a transverse wheel load, as well as the shear stress distributions in the rail. They demonstrated that traditional Hertzian contact theory may not be able to predict the wheel contact stress distributions around rail joints, depending on the material properties of the joint. They revealed that an IJ adhesive with a higher Young's modulus, such as epoxy-fiberglass with a Young's modulus of 6,500 ksi, may result in a more uniform pressure distribution than the two-dimensional parabolic distribution proposed by [1]. The epoxy used in this thesis has a significantly lower Young's modulus, 350 ksi. In their analyses involving epoxies with different material properties, [5] also determined that an epoxy with a lower Young's modulus could result in higher maximum shear stresses in the entire insulated joint, especially when compared to a rail without the presence of an IJ. This increased shear stress was most noticeable at the contact point between the wheel and the top of the insulated joint, and its influence decreases

along the depth of the joint. The location of this maximum shear stress, at the top of the joint bar, can also be seen in the work performed by [8], which describes the mechanical failure of the bond as an "unzipping" of the epoxy initiated at the top of the end post.

Much of the research conducted on the wheel-rail contact problem and Hertz contact theory has focused on the contact between the wheel and the rail, rather than the resulting stresses in the rail and joint. However, the work of [9] did show that variation of the maximum shear stress distribution decreased along the depth of the joint when a Hertz contact patch was used, and since the focus of this analysis is on the stresses found in the adhesive, which is a distance away from the top surface of the rail, the Hertzian contact patch has been used rather than using a single concentrated force to represent the vertical wheel load.

2.2. Rail Foundation

When the analysis of the deformation of rails under wheel loads was first developed, a rail supported by a continuous elastic foundation was used for calculations. With the steadily increasing wheel loads, the steadily decreasing cross tie spacing's, and the increased rail cross sections utilized by the rail industry today, this assumption is enhanced [10]. In his analysis of the rail as a beam on a continuous elastic foundation, used the governing differential equations and solutions proposed (which are discussed in detail in Section 2.2) to determine the deflected shape and resulting bending moments of the rail due to the applied wheel loads. The elastic foundation approach was confirmed by [11], in their analysis of bonded insulated railroad joints, comparing their analytical results to experimental tests of actual bonded joints. One drawback, however, to using an elastic foundation to model ballast and ties supporting a rail is that the springs used to represent the foundation can be in both compression and tension. This means that not only do the elastic foundation springs apply an upward force to rail when it deflects downward, but conversely they can apply a downward force to the rail when the rail deflects upward.

2.3. Ties and Rail Foundation

[12] Analyzed railroad ties to ascertain the effect of wheel loading on ties and subsequently on the supporting ballast and subgrade. In examining the spacing of ties, he determined that decreasing the tie spacing would better distribute the load on the foundation and result in smaller stresses in the foundation. He proposed that the optimum spacing of ties is approximately 19.6 in. to 23.6 in. His analysis also revealed that plastic deformations in ties are negligible and may be ignored, thus elastic behavior can be assumed in analyzing railroad ties. Analysis of multiple ties along the length of the rail showed that the effect of a wheel load when applied directly above a tie is negligible beyond the third successive tie on either side of the point of application

of the load. This means that the effect of a wheel load is only felt by five ties centered about the wheel load.

[13] Determined that the contact pressure between the tie and the ballast may be assumed to be uniform. The effective length of the contact area between the tie and ballast is one-third the total length of the tie under each rail. This effective length is also currently assumed in railroad design.

2.4. Rail Joint Stresses

Rails are produced in fixed lengths and need to be joined end-to-end to make a continuous surface on which trains may run. Prior to about 1970, rails were bolted together by using two joint bars, one on each side of the web with 4 or 6 bolts through the rail track as a geometric requirement. These joint bars have a lower vertical bending stiffness than the straight rail track. As a result; large deflections in the joint region are generated while wheels pass through. The large deflections can accelerate track deterioration. Due to this parts need more research, many researcher are interesting to do their research around this area to solve the problem related to discontinuous of the rail joint to improve the performance, the service life , maintenance cost and to increase the comfort of the passenger. This part deals with previous work is related to the rail joint.

[13] used 3D finite element analysis to study the effect of the discontinuity of the rail ends and the presence of lower modulus insulation material at the gap to the variations of stresses in the insulated rail joint (IRJ) is presented. It is shown that the maximum stress occurs in the subsurface of the railhead when the wheel contact occurs far away from the rail end and migrates to the railhead surface as the wheel approaches the rail end; under this condition, the interface between the rail ends and the insulation material has suffered significantly increased levels of stress concentration. The ratio of the elastic modulus of the railhead and insulation material is found to alter the levels of stress concentration. Numerical result indicates that a higher elastic modulus insulating material can reduce the stress concentration in the railhead but will generate higher stresses in the insulation material, leading to earlier failure of the insulation material.

[14] this paper discusses the effects that track parameters such as foundation configuration and track surface condition have on joint bar stresses. Joint bars were notched using the Electro-discharge machining (EDM) technique to initiate cracks and were tested under controlled conditions at the Facility for Accelerated Service Testing so that crack growth rates under simulated mainline heavy haul freight operations could be evaluated. The limited test data showed no significant difference between concrete and wood tie track in terms of joint bar stresses. However, joints installed in curved track showed a considerable increase in stress state and required more maintenance than joints installed in tangent track. In addition, the data showed that standard joint bars experience higher stresses than insulated rail joints. Similarly,

increasing the number of joint bar bolts and the magnitude of the bolt torque can have positive effects on joint performance. Limited thermal force data showed that insulated joints, once welded in place, behave like the surrounding rail and can develop considerably higher thermal stresses than standard rail joints. After cracks initiated from EDM notches at the bottom of the joint bars on tangent track, two joint bars out of eight broke within 35 million gross tons of traffic.

[15] studied the fatigue life of rail joint bar by using three dimensional finite element model of rail joint bar and dynamic load is applied to estimate the fatigue life of the joint bar. Different component of the rail joint bars are being created separately and assemble in Autodesk Inventor. The model consists of assembly of the rail, joint bars, bolts, nuts, washers, and wheel. A three -dimensional finite element analysis of rail joint bars is carried out in ANSYS after importing from Autodesk Inventor. The static and dynamic loads are being applied to estimate fatigue life and endurance strength at the section. The material properties of the rail and wheel are assumed same. The material properties of the wheel and rail are considered bilinear kinematic hardening in ANSYS.

[16] Investigates an engineering analysis of different designs and failure modes of the IRJ by using a 3D finite element model for analyzing the stresses and strain on rail head. It was present a sensitivity analysis of different joint bar thicknesses (30mm, 34mm, and 40mm) to compare stress and strain distributions on the railhead. It was a small reduction in the stresses encountered by the rail when joined with a pair of joint bars of increased moment of inertia considering the thickness range considered. It suggests that increasing bending stiffness by increasing the thickness of the joint bar is not a good way to reduce stresses and displacements of the rail joint. An important way of increasing bending stiffness of the bar is to increase its height. The increase of stiffness of the bar by increasing height is more dominant compared to that of thickness.

[17] carried a numerical analysis combining dynamic and plastic deformation and material deterioration of IRJ's to investigate the influence of the rail joint on generation of wheel-rail impact load and subsequent material deterioration of the joint. It was argued that these joints form local irregularities and result in a local change of dynamic track stiffness. It was observed that not only the dynamic characteristics of the track by virtue of the presence of the IRJ were altered, but also the surface irregularities caused a high increase in contact load. Consequently, a high stress concentration and a corresponding plastic deformation occurred at the joint.

[18] studied the stress around fish bolt hole by using static loading tests and field tests then compare to stresses were calculated by using FEM. Tensile stress field in the vertical direction occur red when joint bolts were fastened and the maximum stresses were generated at lateral positions of holes. Maximum stress amplitudes were observed at 45-degree position to

longitudinal axis of rail under a vertical load. Based on results, they established a method to evaluate the stresses at the edges of fish bolt holes when fish bolts were fastened and trains passed.

[19] studied change on insulated rail joint design in order to improve the performance of the insulated joint by using finite element method. ABAQUS software is used to model the supported butt joint. In this model, the rail, joint bars, epoxy, and ties surrounding the joint are modeled using solid elements. The remaining ties are modeled as an elastic foundation. The rail is subjected to a tensile load, as well as a vertical wheel load that is applied to the rail using Hertz contact theory. Parametric studied are performed by varying the tie width, joint bar length, and joint bar dimensions. Two different wheel load locations are also investigated: centered about the end post, and halfway between the tie under the end post and the tie just to the left of the end post.

[20] studied the effects of epoxy deboning on the stress and strain are in a bonded insulated joint subjected to longitudinal force. Finite element method is used to model the different type of debonding feature. They studied the effect of the debonding by using Abaqus software. From their result shows under thermal tensile loads, strains at the center of the outer surface of the joint bar tend to increase as debonding begins near the end post. The strain at this point tends to stabilize after the debonding reaches the innermost bolt hole. Strain at a point between the outermost and middle bolt holes starts relatively stable, but increases after debonding passes the innermost bolt hole.

[22] innovative designs for insulated rail joints for improved life cycle and higher cost effectiveness. He is using electrically insulating materials that replace the epoxy used in current bonded insulated joints. Those particular joint design is analyzed structurally using both closed form analysis and FEA analysis using the software package ABAQUS.

Generally stress on rail joints investigated by most researchers however, based on these related researches this study focuses on identifying the stress of rail joints by changing the bolt geometry on the current Ethiopian railway corporation system so that prediction of rail joint stress analysis is done such that the main technical specifications are done specifically with regard to the current Addis Ababa light rail train.

Chapter Three

3. Modeling and analysis of stress on rail joint

3.1. Modeling contact at rail joint

The wheel profile consists of a flange to guide the trains along the rails and a conical tread that contacts rail head, and rail has many curvatures to guide wheel properly. The contact positions of the wheel / rail are different in the different situation. However, this paper uses the contact between the wheels tread and rail head.

The contact area between wheel and rail are very small compared to their dimension.

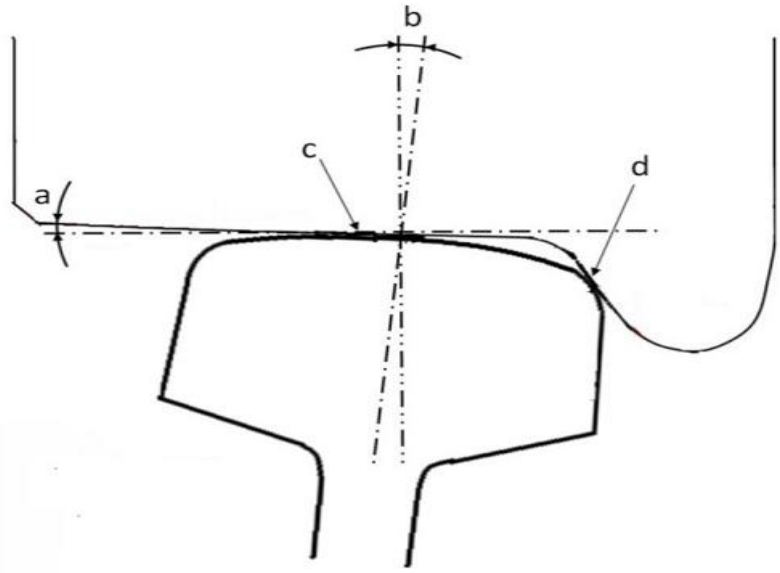

Figure 3.1: Contact zone of wheel/rail.

Rails are produced in fixed lengths and need to be joined end-to-end to make a continuous surface on which trains may run. However, presence of the joint caused the high stress on the rail, which produces the diverse type of wear at the rail head. This paper concerns on the stress distribution on rail joint under vertical wheel load.

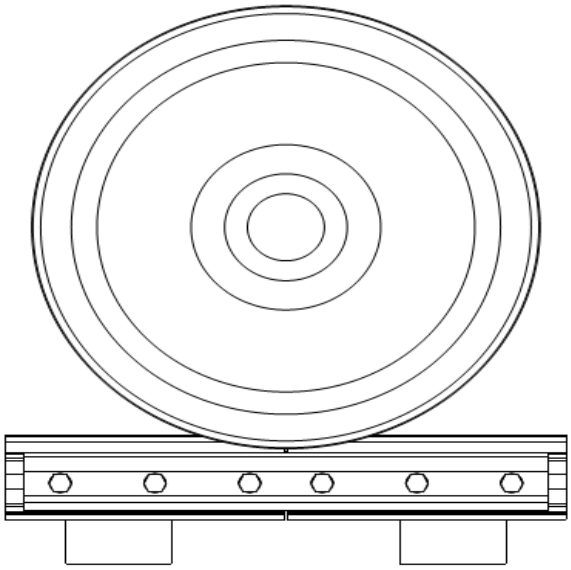

Figure 3.2: wheel rail contact at rail joint.

3.2. Hertz Contact Patch Theory

According to Hertzian contact theory, the contact surface between two curved surfaces, such as a wheel and a rail, can be represented as an ellipse with a major semi-axis a and a minor semi-axis b. The pressure exerted over this elliptical area is parabolic in two directions and is defined according to the following equation:

$$p = p_0\sqrt{1 - \left(\frac{x}{a}\right)^2 + \left(\frac{y}{b}\right)^2} \qquad 3.1$$

Where p_0 is the maximum contact pressure at the initial central contact point, and the coordinates x and y refer to distances from the initial contact point along the major semi-axis and minor semi-axis, respectively. The value of p_0 is given by

$$p_0 = \frac{3}{2}\left(\frac{W}{\Pi ab}\right) \qquad 3.2$$

Where W is the applied normal force.

The magnitudes of a and b also depend on the applied normal force, as well as the profile and materials of the wheel and rail. They are expressed as

$$a = m\left[\frac{3\Pi W(K_1+K_2)}{4K_3}\right]^{1/3} \qquad 3.3$$

$$b = n\left[\frac{3\Pi W(K_1+K_2)}{4K_3}\right]^{1/3} \qquad 3.4$$

Where

$$K_1 = \frac{1-V_W{}^2}{\Pi E_W{}^2} \quad 3.5$$

$$K_2 = \frac{1-V_R{}^2}{\Pi E_R{}^2} \quad 3.6$$

$$K_3 = \frac{1}{2}\left(\frac{1}{R_1} + \frac{1}{R_1{}'} + \frac{1}{R_2} + \frac{1}{R_2{}'}\right) \quad 3.7$$

Here E_W, E_R, V_W, and V_R are the modulus of elasticity and Poisson's ratios of wheel and rail, respectively. R_1 and R_2 are defined as the principal rolling radii of the wheel and rail, respectively. R_1' and R_2' are the transverse radii of curvature of the wheel and rail, respectively.

The coefficients m and n in Equations 3.3 and 3.4 are functions of θ and can be found in a table in [8]. The variable θ is defined as

$$\theta = \cos^{-1}\left(\frac{K_4}{K_3}\right) \quad 3.8$$

Where``

$$K_4 = \frac{1}{2}\left[\left(\frac{1}{R1} + \frac{1}{R_1{}'}\right)^2 + \left(\frac{1}{R_2} + \frac{1}{R_2{}'}\right)^2 + 2\left(\frac{1}{R_1} - \frac{1}{R_1{}'}\right)\left(\frac{1}{R_2} - \frac{1}{R_2{}'}\right)\cos 2\varphi\right] \quad 3.9$$

And φ is the angle between the normal planes that contain the curvatures 1/R1and 1/R2 [14].

3.3. Finite element theory for Contact body

Finite element theory is used to show that relationship among the contact force, applied force, support and free displacement of wheel /rail contact. During the formulations of finite element the contact between the wheel and rail is assumed:

- Isotropic
- Homogeneous
- Linear elastic body Ω with boundary conditions

The linear elastic bodies have four boundaries condition as shown in the figure below.

- Γ_1 is the boundary with zero displacement.
- Γ_2 is the boundary where measured displacements.
- Γ_3 is the boundary with unknown contact forces Fc and unknown contact deformation or displacements.
- Γ_4 is the boundary where applied forces Fa and the other are free surface except those mentioned above. The displacements on boundary Γ4 are unknown.

Let's recall the general form of static finite element system, which is

$$KU=F \text{ [5]} \quad 3.10$$

K, U and F are stiffness matrix of the system, nodal vector displacement, and nodal vector forces. According to the classification of the boundary, it constructs the finite element equation in the following form:

$$\begin{bmatrix} K_{11} & K_{12} & K_{13} & K_{14} \\ K_{21} & K_{22} & K_{23} & K_{24} \\ K_{31} & K_{32} & K_{33} & K_{34} \\ K_{41} & K_{42} & K_{43} & K_{44} \end{bmatrix} \begin{bmatrix} U_1 \\ U_2 \\ U_3 \\ U_4 \end{bmatrix} = \begin{bmatrix} F_1 \\ F_2 \\ F_3 \\ F_4 \end{bmatrix} \qquad 3.11$$

K_{ij} and F_1 are sub-stiffness matrix and vector of reaction forces on the boundary Γ_1.

F_2 is a vector forces on the boundary Γ_2 with measured displacements, usually there is no force on the measured boundary. F_c and F_a is vector of unknown reaction or contact forces on the boundary Γ_3 and vector of known applied forces on the boundary Γ_4.

U_1 and U_2 are known displacements on constrained boundary Γ_1 and measured displacement on free boundary Γ_2.

U_3 and U_4 are unknown displacements on contact boundary Γ_3 and unknown displacements on boundary Γ_4 with known applied force F_a, the free surface with no applied force and the internal nodes where net force is zero.

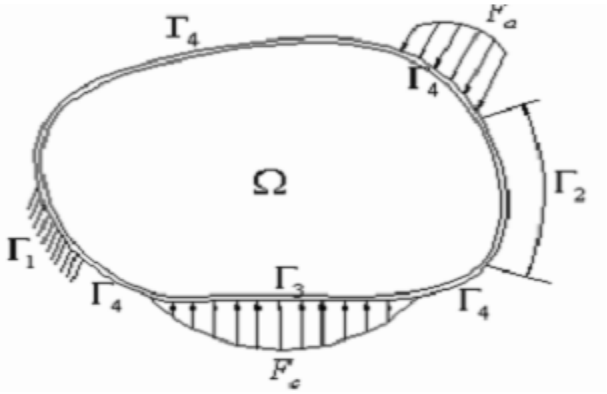

Figure 3.3: Contact model analyze [16].

The stiffness matrix is singular and no unique solution for displacement is possible if the structure is unsupported for the above structure stiffness equation. For this reason all displacement on the boundary Γ_1 are zero that means U_1=0.When apply this condition to the system matrix and vector in equation 3.11 FEA equation becomes:

$$\begin{Bmatrix} K_{22} & K_{23} & K_{24} \\ K_{32} & K_{33} & K_{34} \\ K_{42} & K_{43} & K_{44} \end{Bmatrix} \begin{Bmatrix} U_2 \\ U_3 \\ U_4 \end{Bmatrix} = \begin{Bmatrix} F_2 \\ F_c \\ F_a \end{Bmatrix} \quad 3.12$$

To calculate the contact forces F_c at U_2. Multiple 3rd row of the stiffness matrix with displacement matrix, then equation became:

$$K_{42}U_2 + K_{43}U_3 + K_{44}U_4 = Fa \quad 3.13$$

$$U4 = K_{44}^{-1}[F_a - K_{42}U_2 - K_{43}U_3] \quad 3.14$$

Multiple the 2nd rows with displacement column, the equation became;

$$K_{32}U_2 + K_{33}U_3 + K_{34}U_4 = Fc \quad 3.15$$

$$U_3 = K_{33}^{-1}[F_3 - K_{32}U_2 - K_{34}U_4] \quad 3.16$$

When equation 3.13 substitute in the equation 3.14, U_3 became;

$$U3 = K_{33}^{-1}[F_c - (K_{33} - K_{34}K_{44}^{-1}K_{43})U_2 - K_{34}K_{44}^{-1}F_a + K_{34}K_{44}^{-1}K_{43}U_3] \quad 3.17$$

Therefore the displacement at the contact point is:

$$U3 = K_{33}^{-1}[F_c - (K_{33} - K_{34}K_{44}^{-1}K_{43})U_2 - K_{34}K_{44}^{-1}F_a + K_{34}K_{44}^{-1}K_{43}U_3] \quad 3.18$$

Generally, the contact between the wheel and rail are considered to determining the failure effect of rail end and rail joint.

Stress -strain relationship of structural analysis

$$\{\sigma\} = \{K\}\{\epsilon^{el}\} \quad 3.19$$

ϵ^{el}, σ and D are elastic strain vector, stress vector and elastic stiffness matrix.

$$\{\sigma\} = \{\sigma_x, \sigma_y, \sigma_z, \sigma_{xy}, \sigma_{yz}, \sigma_{xz}\} \quad 3.20$$

$$\{\epsilon^{el}\} = \{\epsilon\} - \{\epsilon\}^{th} \quad 3.21$$

$$\{\epsilon\} = \{\epsilon\}^{th} + \{D^{-1}\} + \{\sigma\} \quad 3.22$$

$$\{D^{-1}\} = \begin{bmatrix} 1/E_x & -v_{xy}/E_x & -v_{xy}/E_x & 0 & 0 & 0 \\ -v_{yx}/E_y & 1/E_y & -v_{yz}/E_y & 0 & 0 & 0 \\ -v_{zx}/E_z & -v_{zy}/E_z & 1/E_z & 0 & 0 & 0 \\ 0 & 0 & 1/G_{xy} & 0 & 0 & 0 \\ 0 & 0 & 0 & 1/G_{yz} & 0 & 0 \\ 0 & 0 & 0 & 0 & 0 & 1/G_{xz} \end{bmatrix} \quad 3.23$$

E_x and G_{xy} are young's modulus in the x direction and shear modulus in the xy plane V_{xy} and v_{yx} are major poison's ratio and minor poison's

Also the $\{D^{-1}\}$ matrix is presumed to be symmetric, so that

$$\frac{v_{xy}}{E_Y} = \frac{v_{xy}}{E_x} \quad 3.24$$

$$\frac{v_{zx}}{E_z} = \frac{v_{xz}}{E_x} \quad 3.25$$

$$\frac{v_{zy}}{E_z} = \frac{v_{yz}}{E_x} \quad 3.26$$

$$\frac{v_{zx}}{E_z} = \frac{v_{xz}}{E_x} \quad 3.27$$

$$\frac{v_{zy}}{E_z} = \frac{v_{yz}}{E_y} \quad 3.28$$

The element integration point strain and stress are:

$\{\epsilon^{el}\} = \{B\}\{U\} - \{\epsilon\}^{th}$, for this case, $\{\epsilon\}^{th}$ is zero. 3.29

$\{\sigma\} = \{D\}\{\epsilon^{el}\}$ 3.30

B and $\{\epsilon\}^{th}$ are strain - displacement matrix evaluated at integration point and thermal strain

ϵ^{el} Is strain that cause stress

Maximum stress failure criteria

$$\varepsilon_x = \text{Maximum of } \begin{cases} \frac{\sigma_{xc}}{\sigma^f{}_{xc}} & , \frac{\sigma_{xy}}{\sigma^f{}_{xy}} \\ \frac{\sigma_{yc}}{\sigma^f{}_{yc}} & , \frac{\sigma_{yz}}{\sigma^f{}_{yz}} \\ \frac{\sigma_{zc}}{\sigma^f{}_{zc}} & , \frac{\sigma_{zx}}{\sigma^f{}_{zx}} \end{cases} \quad 3.31$$

$\sigma_x, \sigma_y \; and \; \sigma_z$ Are stresses in x, y, and z direction.

$\sigma^f{}_{xc}, \sigma^f{}_{yc}$ and $\sigma^f{}_{zc}$ Are normal stress failures in x, y and z direction.

$\sigma_{xy}, \sigma_{yz}, \; and \; \sigma_{xz}$ are shear failure in xy, yz, and xz direction.

3.4. Material Selection

3.4.1. Rail Material Selection

Rails are grouped according to their standards, strength, grade, quality and length. The rail steel qualities can be distinguished in to two categories.

- Normal steel quality, with an ultimate tensile strength of 700-900 MPa
- Hard steel quality, used mainly on curves, and crossings etc. with an ultimate tensile strength of 900-1200 MPa

Concerning their chemical compositions rails have great varieties of carbon, manganese, chromium and silicon contents depending on their requirements. Since the rails have to withstand the impact load, friction and stress of freights, they should have sufficient strength, hardness, toughness and good welding performance. However a large increase in rail mechanical strength may result brittle failure and as a result a further increase is not desirable. Similarly, the same material property is selected for wheel materials.

Rail Stresses

Bending Stress – Bending of the rail that occurs from vertical wheel loading and lateral wheel loading. Vertical wheel loading normally results from loading between the tie supports, and causes tensile longitudinal stresses in the rail base area and head/web fillet area. Lateral wheel

loading applies tensile longitudinal stresses in the rail web area and head/web area of the rail field side.

Thermal Stress – These stresses occur in continuous welded rails due to thermal expansion and contractions that occur as the actual rail temperature increases above or reduces below the rail neutral temperature. When the rail temperature is above neutral temperature, compressive longitudinal stresses are established. When the rail temperature is below neutral temperature, tensile longitudinal stresses are established. These stresses can drastically influence rail flaw development.

Residual Stress – These stresses are a result of the manufacturing process, particularly from roller straightening and head hardening. They can also result from the welding of rails because of the different expansion and contraction of the steel that occurs during the weld process. Residual stresses can be found in any location within the rail section and can exhibit high tensile stresses that can result in rail failure.

Table 3.1: Mechanical property of rail material

S.N	Mechanical property	Value
1	Poison's Ratio	0.3
2	Young's Modulus (GPa)	207
3	Ultimate tensile strength (MPa)	780
4	Yield strength (Mpa)	640
5	Density (Kg/m)	7800
6	Elongation	12%

3.4.2. Wheel Material Selection

A railway wheel, together with an axle, is one of the crucial parts that support the safe operation of railway vehicles. Wheels support the entire weight of cars; however, they cannot be designed as a failsafe structure where a backup system by other parts can be applied in case of a serious problem. Therefore, absolutely high reliability is demanded in terms of strength. Accordingly, the most important and fundamental characteristic in designing wheels is strength. However, since "being unbreakable" is a significant wheel characteristic, from the viewpoint of advantageous performance, characteristics other than strength, such as wear resistance, thermal crack resistance, and noise/vibration, are often focused. In particular, since wheels are

expendable parts, their life plays a significant role in saving the maintenance cost. In order to improve these characteristics, up to now, various studies have been conducted and technological developments have been made. There are mainly two approaches to improve the wheel performance: material designing and configuration designing.

Table 3.2: Mechanical property of wheel material

S.N	Mechanical property	Value
1	Poison's Ratio	0.3
2	Young's Modulus (GPa)	207
3	Ultimate tensile strength (MPa)	780
4	Yield strength (Mpa)	640
5	Density (Kg/m)	7800
6	Elongation	12%

3.4.3. Fish plate material

The function of the fishplate is to hold the two rails together both in the horizontal and vertical planes. The fish plates are manufactured from a special type of steel having composition of Carbon, Manganese, Silicon, Sulphur and Phosphorous 0.30 to 0.42%, Not more than 0.8%, Not more than 0.15%, Not more than 0.06 % respectively. The fish plates are so designed that the fishing angles at the top and bottom surface coincide with those of the rail section so as to have a perfect contact with the rail.

Table3.3: Mechanical property of fishplate.

S.N	Mechanical property	Value
1	Poison's Ratio	0.3
2	Young's Modulus (GPa)	207
3	Ultimate tensile strength (MPa)	780
4	Yield strength (Mpa)	640
5	Density (Kg/m)	7800
6	Elongation	12%

3.4.4. Bolt Materials

Over 90% of fasteners manufactured use carbon steel. Steel has excellent workability, offers a broad range of attainable combinations of strength properties, and in comparison with other commonly used fastener materials, and is less expensive.

The mechanical properties are sensitive to the carbon content, which is normally less than 1.0%. For fasteners, the more common steels are generally classified into three groups: low carbon, medium carbon and alloy steel.

i. Low Carbon Steels

Low carbon steels generally contain less than 0.25% carbon and cannot be strengthened by heat-treating; strengthening may only be accomplished through cold working. The low carbon material is relatively soft and weak, but has outstanding ductility and toughness; in addition, it is Machinable, weldable and is relatively inexpensive to produce. The most commonly used chemical analyses include AISI 1006, 1008, 1016, 1018, 1021, and 1022.

Table 3.4: Mechanical property low carbon steel

S.N	Mechanical property	Value
1	Poison's Ratio	0.3
2	Young's Modulus (GPa)	207
3	tensile strength (MPa)	482
4	Yield strength (Mpa)	302
5	Density (Kg/m)	7800
6	Elongation	25%

ii. Medium Carbon Steels

Medium carbon steels have carbon concentrations between about 0.25 and 0.60 wt. These steels may be heat treated by austenizing, quenching and then tempering to improve their mechanical properties. The plain medium carbon steels have low hardenabilities and can be successfully heat-treated only in thin sections and with rapid quenching rates. This means that the end properties of the fastener are subject to size effect.

On a strength-to-cost basis, the heat-treated medium carbon steels provide tremendous load carrying ability. They also possess an extremely low yield to tensile strength ratio; making them very ductile. The popular chemical analyses include AISI 1030, 1035, 1038, and 1541.

Table 3.5: Mechanical property medium carbon steel

S.N	Mechanical property	Value
1	Poison's Ratio	0.3
2	Young's Modulus (GPa)	207
3	tensile strength (MPa)	740
4	Yield strength (Mpa)	490
5	Density (Kg/m)	7800
6	Elongation	20%

iii. Alloy Steels

Carbon steel can be classified as alloy steel when the manganese content exceeds 1.65%, when silicon or copper exceeds 0.60% or when chromium is less then4%. Carbon steel can also be classified as an alloy if a specified minimum content of aluminum, titanium, vanadium, nickel or any other element has been added to achieve specific results. Additions of chromium, nickel and molybdenum improve the capacity of the alloys to be heat treated, giving rise to a wide variety of strength to ductility combinations.

Table 3.6: Mechanical property of alloy steel

S.N	Mechanical property	Value
1	Poison's Ratio	0.3
2	Young's Modulus (GPa)	207
3	Ultimate tensile strength (MPa)	780
4	Yield strength (Mpa)	640
5	Density (Kg/m)	7800
6	Elongation	12%

iv. Stainless Steel

Stainless steel is a family of iron-based alloys that must contain at least 10.5% chromium. The presence of chromium creates an invisible surface film that resists oxidation and makes the material "passive" or corrosion resistant. Other elements, such as nickel or molybdenum are added to increase corrosion resistance, strength or heat resistance.

Stainless steels can be simply and logically divided into three classes on the basis of their microstructure; austenitic, martensitic or ferritic. Each of these classes has specific properties and basic grade or "type." Also, further alloy modifications can be made to alter the chemical composition to meet the needs of different corrosion conditions, temperature ranges, strength requirements, or to improve weld ability, machinability, work hardening and formability.

Austenitic stainless steels contain higher amounts of chromium and nickel than the other types. They are not hardenable by heat treatment and offer a high degree of corrosion resistance. Primarily, they are nonmagnetic; however, some parts may become slightly magnetic after cold working. Stainless steel is a type of austenitic stainless steel that contains approximately 18% chromium and 8% nickel.

Table 3.7: Mechanical property of stainless steel

S.N	Mechanical property	Value
1	Poison's Ratio	0.3
2	Young's Modulus (GPa)	207
3	tensile strength (MPa)	586
4	Yield strength (Mpa)	207
5	Density (Kg/m)	7750
6	Elongation	12%

3.5. Method

3.5.1. The numerical model

As shown in fig.3.4, a 3D finite element model was set up for the time domain simulation of a wheel rolling over a joint with the speed v. A half of a wheel set was modeled with a section of railway track of 1 meters long. The wheel-rail geometry corresponds to Addis ababa LRT with a radius of 0.35 meter; the rail is modeled as UIC60 with an inclination of 1:20. The joint position is at the middle of the wheel.

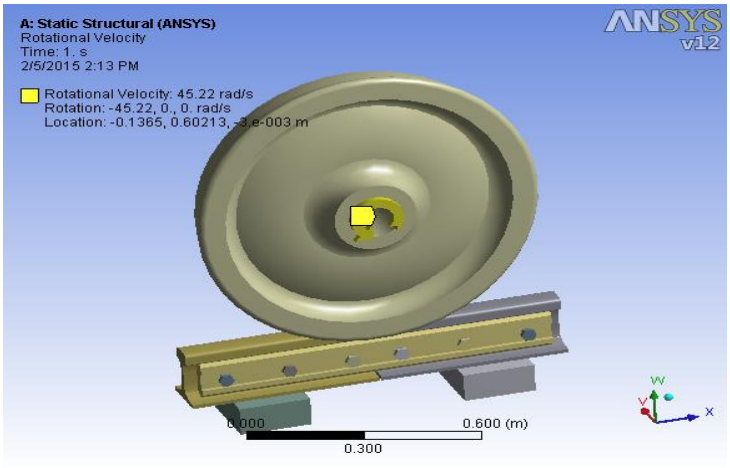

Figure 3.4: a wheel roll on the joint with speed v.

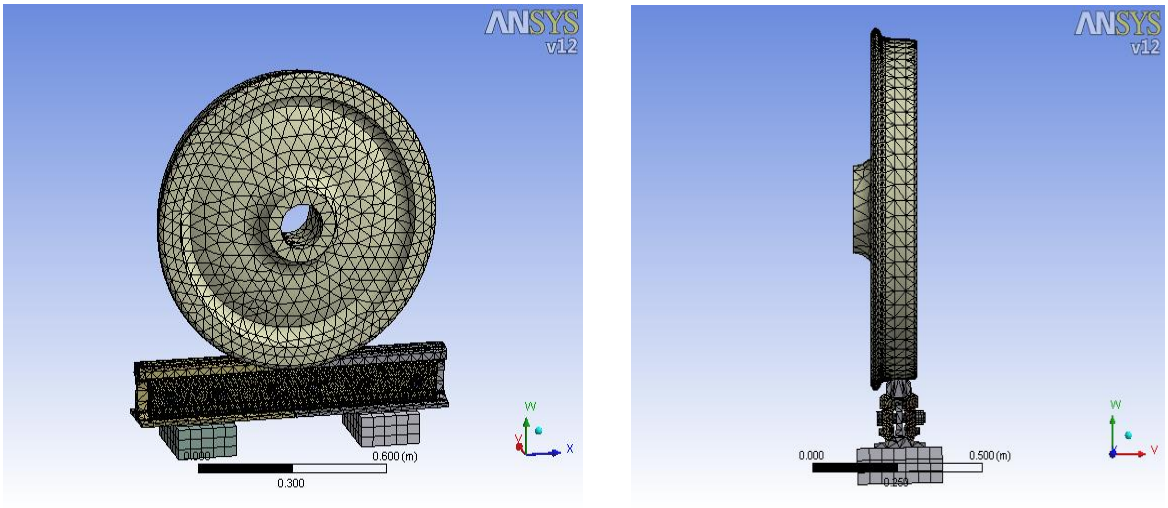

Figure 3.5 the 3D finite element model

3.6. Wheel/rail Contact Simulation

3.6.1. 3D model of rail joint

As discus on above portion, rail joint is a critical component of the railway track infrastructure. For this reason, it needs careful analysis to protect the rail joint. Standard bolted joint contains rail, joint bars, bolts; nuts and washers are used to secure fastening assembly. The assembly is done on the modeling package of CATIAV5R16. CATIAV5R16 is 3D mechanical design software for creating 3D prototypes, used to design, visualize and simulate of the analysis.

Figure 3.6: Three dimensional model of wheel/rail at rail joint.

Assembly model created in assemble workbench of the CATIA after each component of joints created on part of work bench. The assembly model consists; rails, joint plates, bolts, nut,

washer, and wheel. The dimensions and specifications of each part are based on the Ethiopian railway.

Table 3.8: Dimensions and Specification

Item No	Description	Dimension
1	Type of rails for main lines and depot	60kg/m
2	Track gauge:	1435
3	Wheel diameter (new wheel)	700mm
4	Fish Plate length	940mm
5	Plate thickness	45mm
6	Sleeper space	600mm
7	End gap	6mm

3.6.2. Finite element model

For all of the finite element models built using ANSYS to represent the railroad joint, a single UIC60 rail with standard joint bar was used. The UIC60 rail has a moment of inertia of 4.14xe-5m^4, and two standard joint bars have a combined moment of inertia of 1.04x10e-5m^4. The rail, wheel, and joint bars are made of steel, which has a Young's modulus of 2.1Gpa and a Poisson's ratio of 0.3. The rail was subjected to a vertical wheel load of 45kN. Solid linear tetrahedral elements (designated C3D4) were used in the mesh in order to accurately represent the curved surfaces of the rail and joint bars. The material properties are all consistent with earlier work done on this project.

3.6.3. Steps for finite element analysis:

FEA is mainly divided into three following stages:

• Preprocessing

- Creating the model.
- Defining the element type
- Defining material properties
- Meshing
- Applying loads

- Applying boundary conditions

• Solution: Assembly of equations and obtaining solution

• Post processing: Review of results such as deformation plot, stress plot, etc.

3.6.4. The sleepers

In the finite element models of the railroad joints developed in this research, two sleepers are to be placed beneath the end post in between. Two sleepers were modeled as solid elements. The dimensions of the sleeper used in the models are 190mm x 90mm x 250mm. sleepers are spaced 600 mm apart.

The sleeper used in the model is to be concrete.

Figure 3.7: Addis Ababa LRT sleeper.

3.6.5. Finite Element model of Joint Bar:

The analysis of the joint bar model consists of three major steps of defining the geometry and material, loading and boundary conditions. Geometry: The cross section of the joint assembly is depicted in "Figure 3.3". A 3D model of 6-bolt joint bar with some partitions is depicted in "Figure 3.4". The cross section of the joint bar is shown in "Figure 3.5". The left hand side of the bar is laid on the rail.

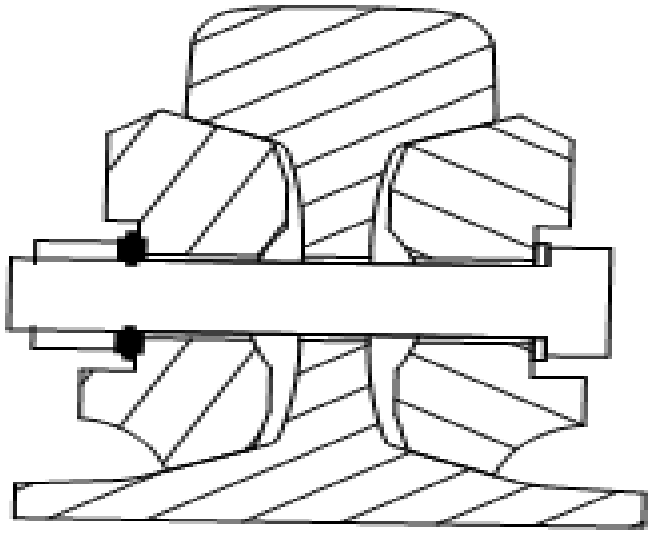

Figure 3.8: rail joint assembly cross section.

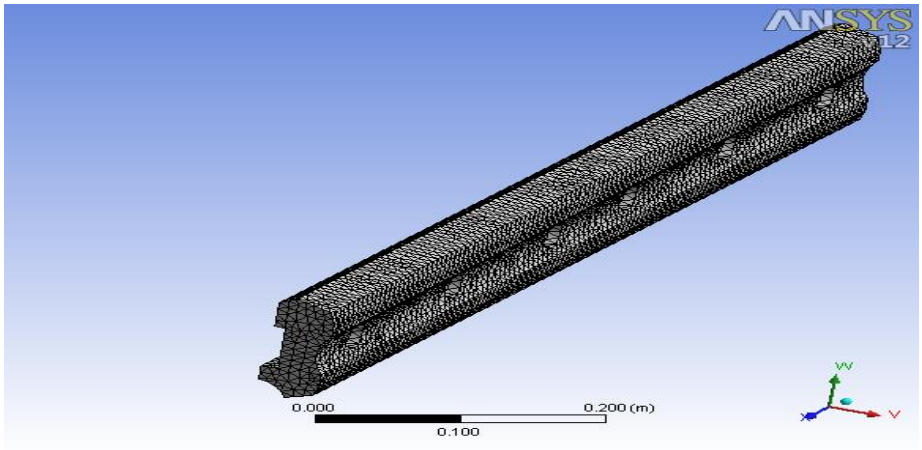

Figure 3.9: geometry of joint bar with some partition.

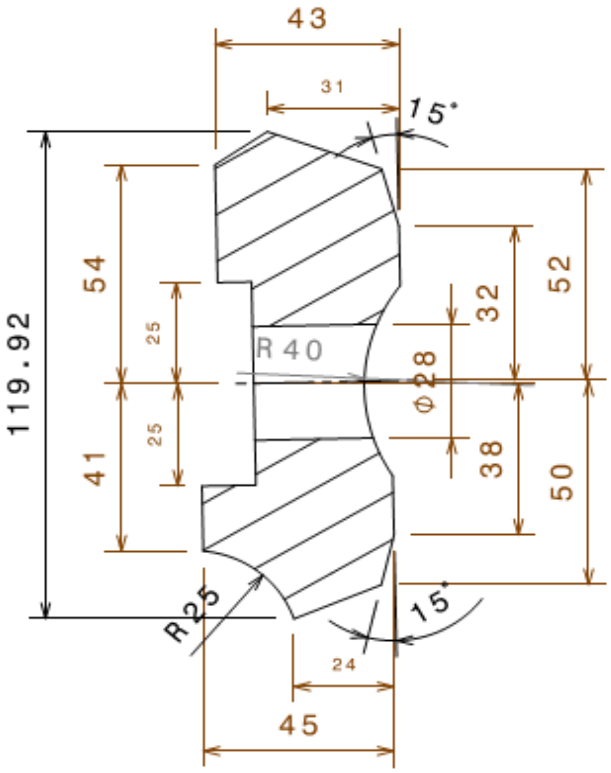

Figure 3.10: geometry of the cross section of joint bar.

3.6.6. Finite element model of the bolt

The finite element models of the rail joint bolts are established. According to the national standards, the material of the bolts is steel whose Young's modulus is 207 Gpa, Poisson's ratio is 0.3, yield strength is 740Mpa and tensile strength is 862Mpa. The geometry dimension of the bolt as follows:

1. M22 the length of bolt bar is 135mm, the nominal diameter with screw thread is 22mm, the length of the thread is 56mm, the thread pitch is 2.5mm.
2. M24 the length of the bolt bar is 128, the nominal diameter is 24mm, the length of the thread is 60mm, and the pitch is 3mm.
3. M27 the length of the bolt bar is 128, the nominal diameter is 27mm, the length of the thread is 60mm, and the pitch is 3mm.

3.6.7. Bolt size

Bolt geometry's are considered to examine their effects on the stress in the joint they are hexagonal head, oval head, and square head. The wheel load was placed at the end post, i.e., at the center of the railroad joint, for all cases, as shown below in Figure 3.8. as the wheel load moves toward a rail end, larger plastic zones with increased von Mises stresses occur in the rail, which could cause deterioration of the rail end.

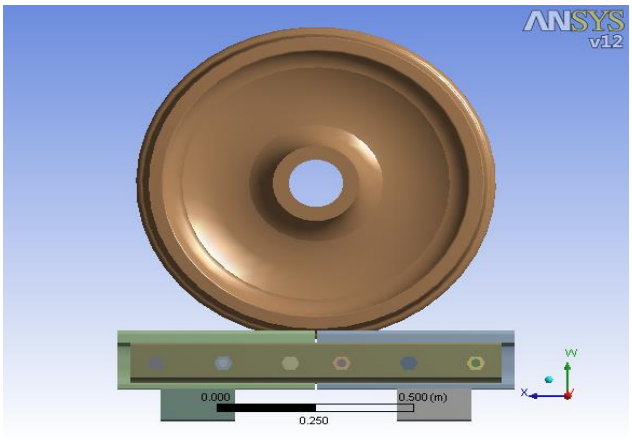

Figure 3.11: rail joint with M24 joint bar, load at end post

3.6.8. M22 bolt

As shown in the figure 3.12 the wheel, rail, joint bar, bolt assembly is modeled and the bolt size is shown in fig.3.13

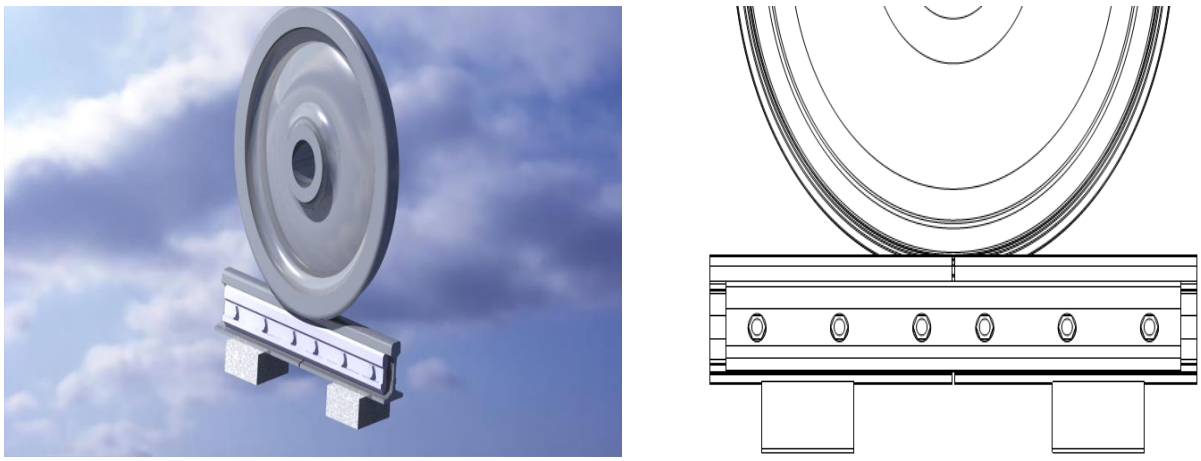

Figure 3.12: wheel, rail, joint, and M22 bolt model.

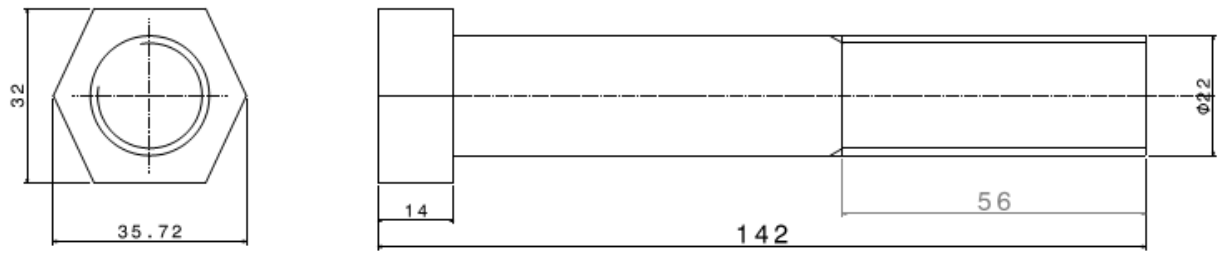

Figure 3.13: the geometry M22 bolt.

3.6.9. M24 bolt

As shown in the figure 3.14 the wheel, rail, joint bar, bolt assembly is modeled and the bolt size is shown in fig.3.15

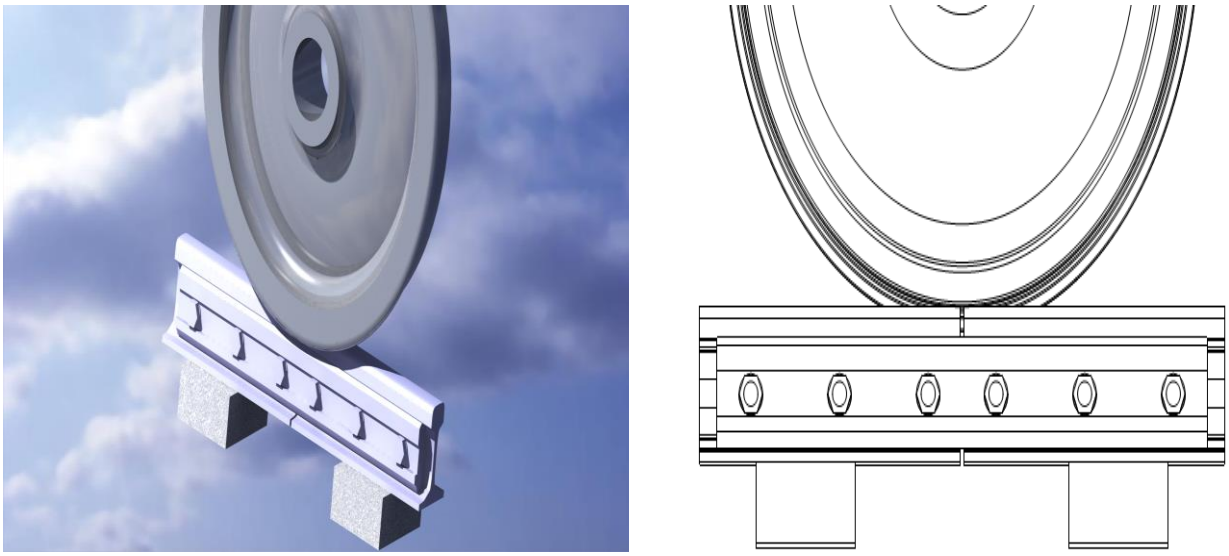

Figure 3.14: wheel, rail, joint and M24 bolt model.

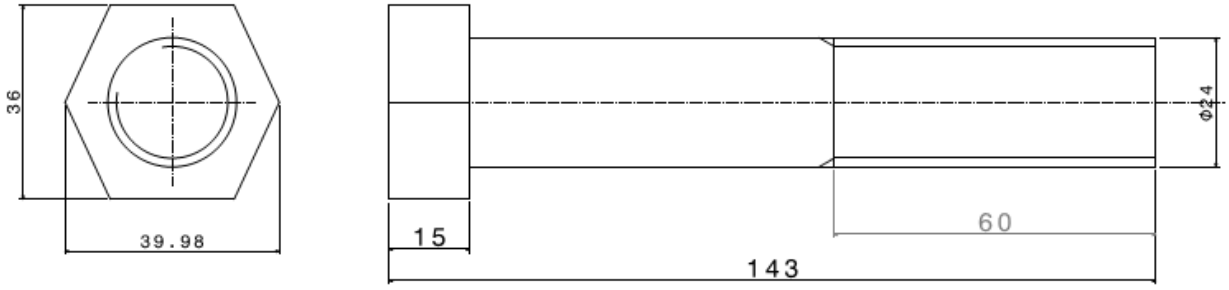

Figure 3.15: the geometry of M24 bolt.

3.6.10. M27 bolt

As shown in the figure 3.16 the wheel, rail, joint bar, bolt assembly is modeled and the bolt size is shown in fig.3.17

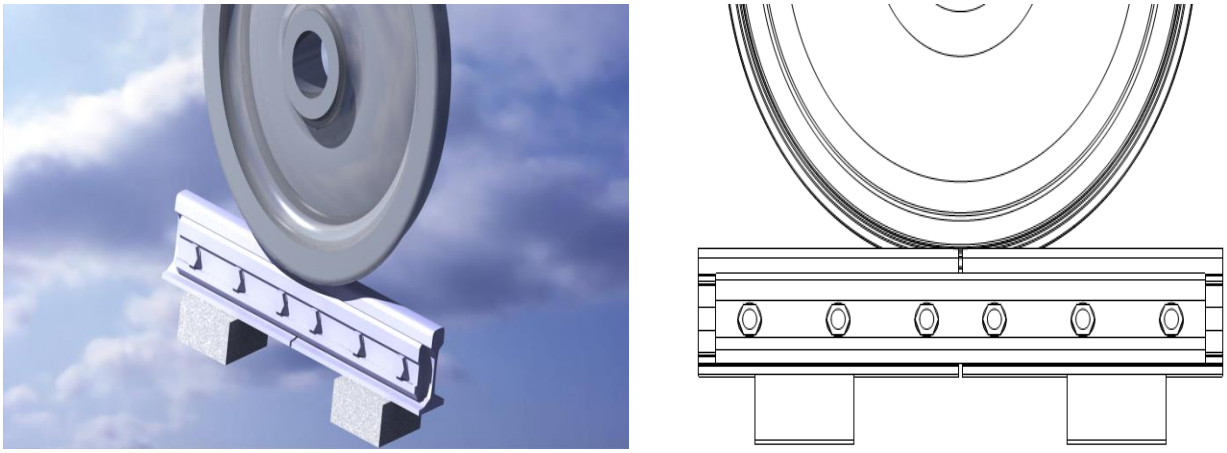

Figure 3.16: wheel, rail, joint and M27 bolt model.

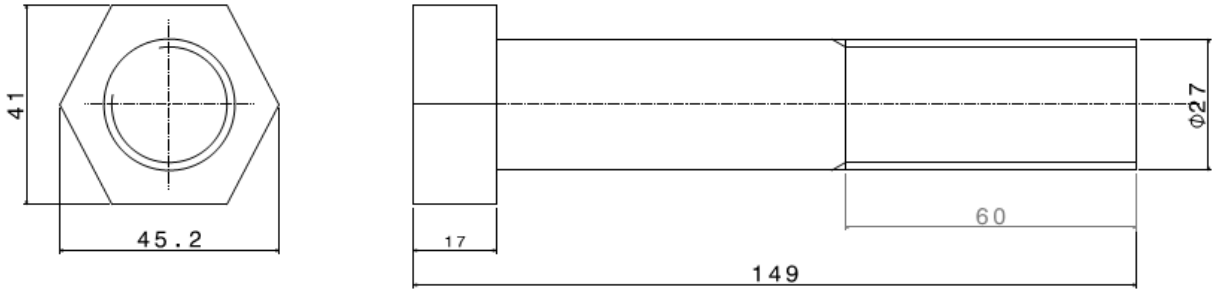

Figure 3.17: the geometry M27 bolt.

3.7. Boundary conditions

All the material properties and boundary conditions are being applied strictly as per the data obtained from the Ethiopian Railways. The wheel runs at constant speed of 70 km/hr., 45.22rad/s. UIC 60 rail is used for analysis. The diameter of wheel is 700mm. The axle load is 90KN. The material's density is 7800 kg/m3. Material properties of the rail and wheel are assumed to be same. The material properties of the wheel and rail are considered to be bilinear kinematic hardening in ANSYS. Fig.3.16 shows boundary conditions and load conditions on rail joint bar.

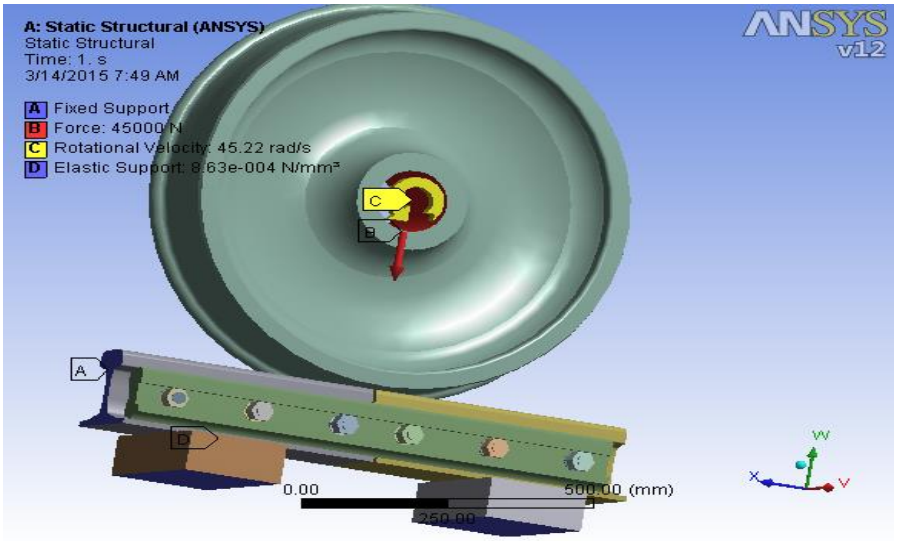

Figure 3.18: boundary and load condition.

Chapter Four

4. Result and discussion

4.1. Result

As stated earlier, this research focuses on the stresses in the joint. For all finite element models of the joint analyzed, and stresses are compared to determine the influence of bolt geometry bolt material on the joint performance.

i. Bolt geometry

Case 1: When M22 bolt geometry is used.

A. Equivalent (von- mises) stress(MPa)

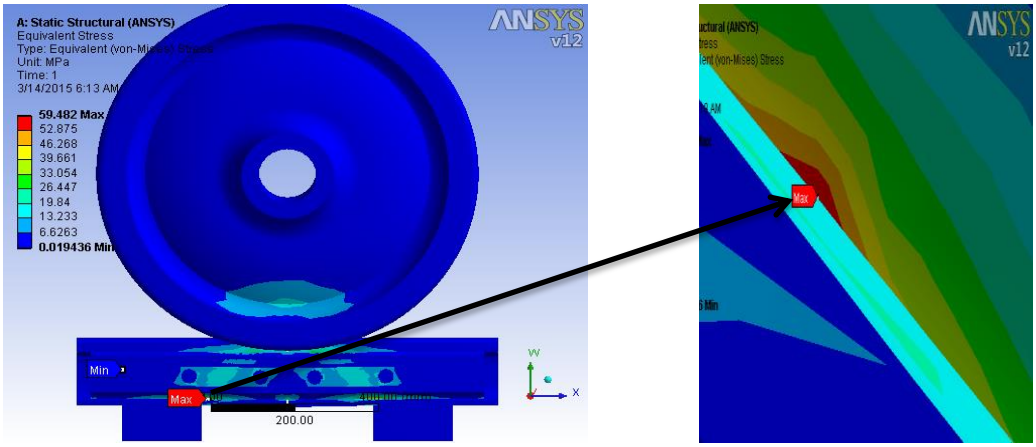

Figure 4.1: equivalent stress on the joint when M22 bolt is used.

From the ANSYS result when M22 bolt is used the equivalent stress is as shown in figure 4.1: the maximum stress is 59.482Mpa and the minimum is 0.019436pa.

B. shear stress

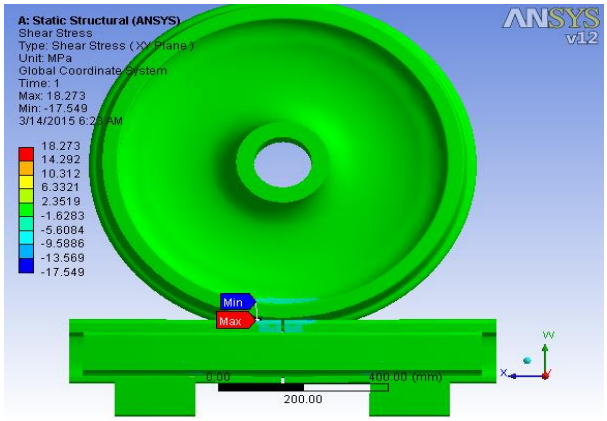

Figure 4.2: shear stress when M22 bolt is used.

And the shear stress is shown in the figure 4.2: the maximum shear stress is 18.273Mpa, and the minimum shear stress is -17.549Mpa.

C. Normal stress(bending stress)(MPa)

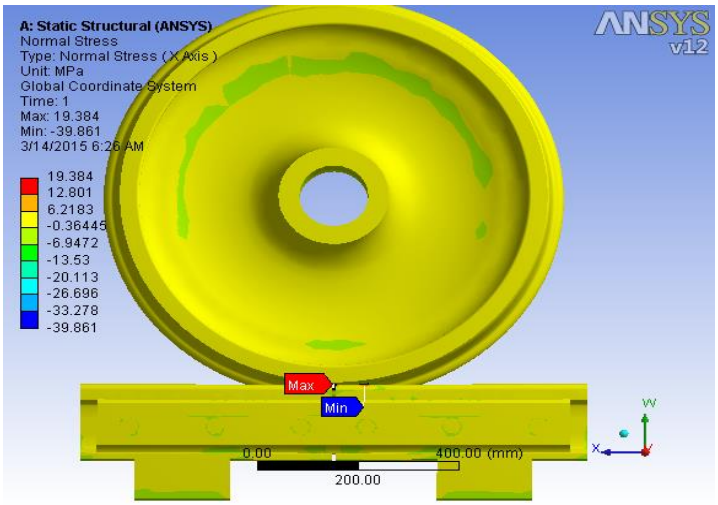

Figure 4.3: Normal stress when M22 bolt is used.

As shown in above figure 4.3: the maximum normal stress is 19.384MPa and the minimum normal stress is -39.861MPa, when M22 bolt is used.

D. Factor of safety

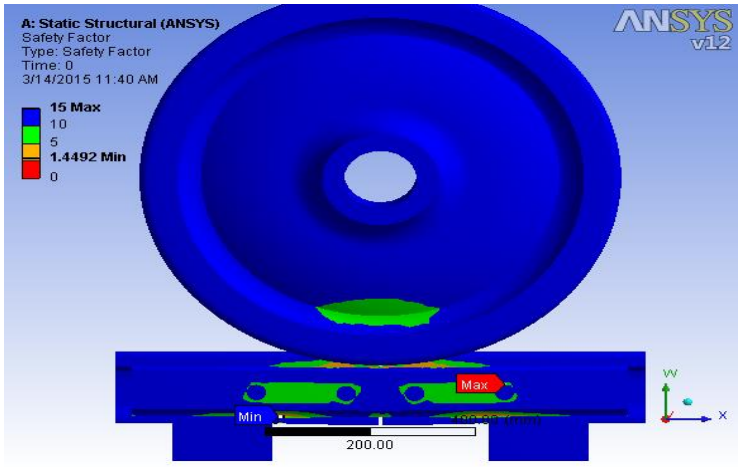

Figure 4.4: factor of safety when M22 bolt is used.

As shown in above figure 4.4, the maximum safety factor is 15 and the minimum safety factor is 1.7418, when M27 bolt is used.

E. Stress on the fish plate and bolt.

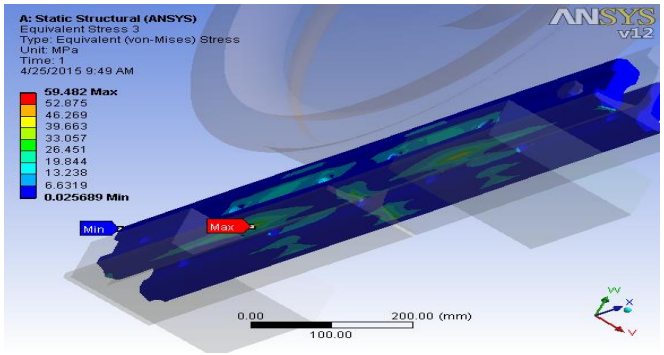

Figure: 4.5 equivalent stresses on the fish plate when M22 bolt is used.

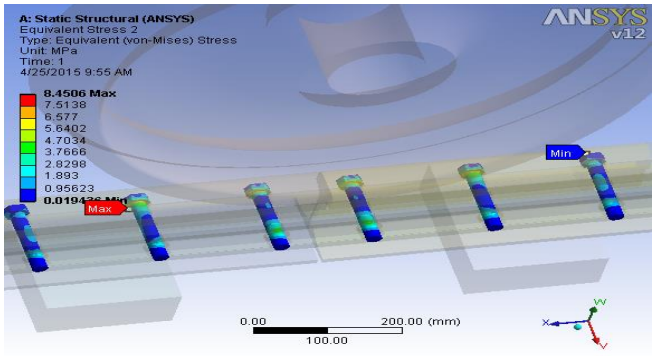

Figure: 4.6 equivalent stresses on the bolt when M22 bolt is used.

Case 2: When M24 bolt geometry is used.

A. Equivalent (von- mises) stress(MPa)

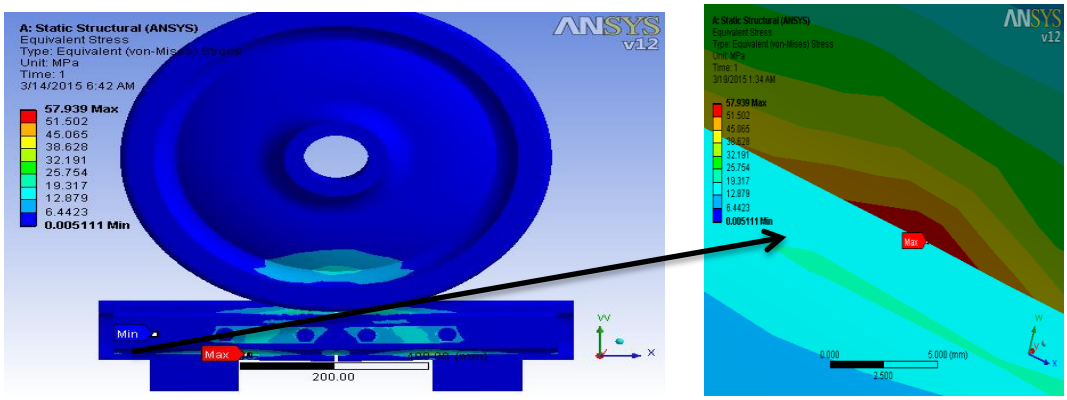

Figure: 4.7 equivalent stresses on the joint when M24 bolt is used.

When M24 bolt is used the ANSYS result of the equivalent stress is shown in the figure 4.5: the maximum stress is 57.939Mpa and the minimum is 0.005111pa.

B. Shear stress (Mpa)

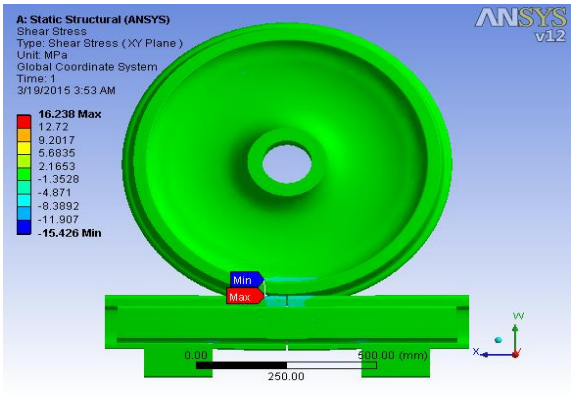

Figure 4.8: shear stress when M24 bolt is used.

And the shear stress is shown in the figure 4.6: the maximum shear stress is 16.238Mpa, and the minimum shear stress is -15.426Mpa.

C. Normal stress (bending stress) (MPa)

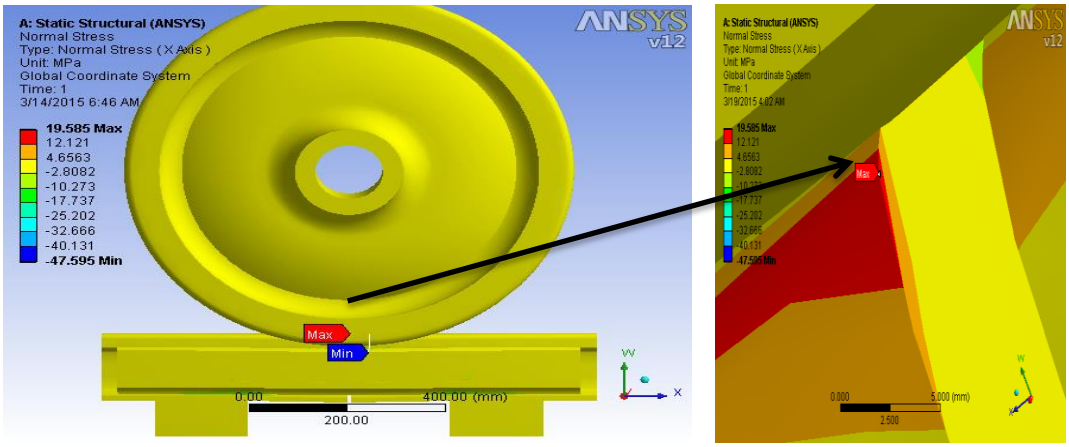

Figure 4.9: normal stress when M24 bolt is used.

As shown in above figure 4.7: the maximum normal stress is 19.585MPa and the minimum Normal stress is -47.595MPa, when M24 bolt is used.

D. Safety factor

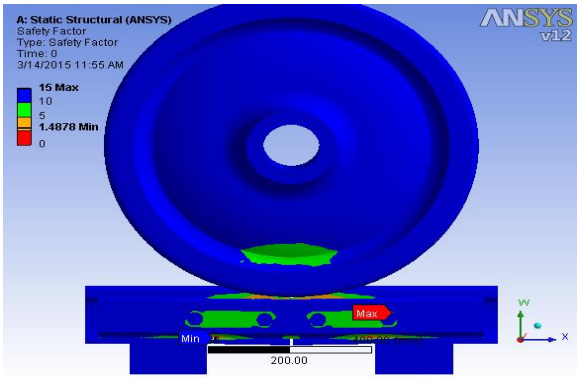

Figure 4.10: safety factor when M24 bolt is used.

As shown in above figure 4.10: the maximum safety factor is 15 and the minimum safety factor is 1.4878, when M24 bolt is used.

E. Stress on the fishplate and bolt

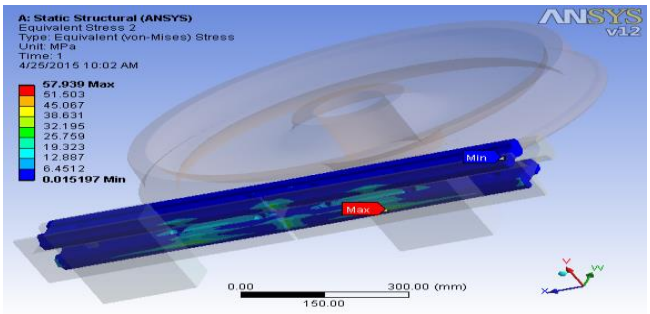

Figure 4.11: equivalent stress on the fish plate when M24 bolt is used.

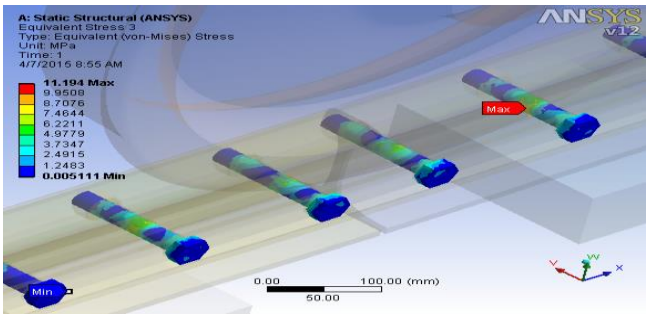

Figure 4.12: equivalent stress on the bolt when M24 bolt is used

Case 3: When M27 bolt geometry is used.

A. Equivalent (von- mises) stress(MPa)

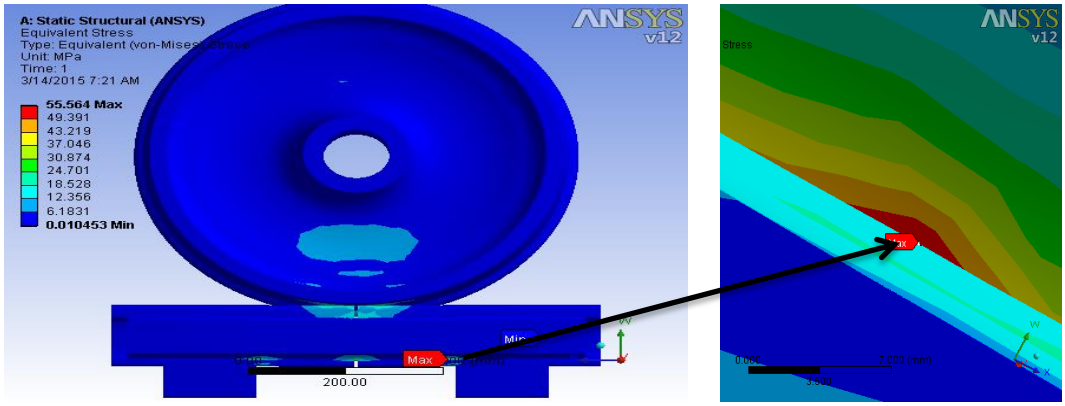

Figure 4.13: Equivalent stress on the joint when M27 bolt is used

When M27 bolt is used the ANSYS result of the stress is shown in the figure 4.13: the maximum equivalent stress is 55.564Mpa and the minimum is 0.010453pa.

B. Maximum Shear stress

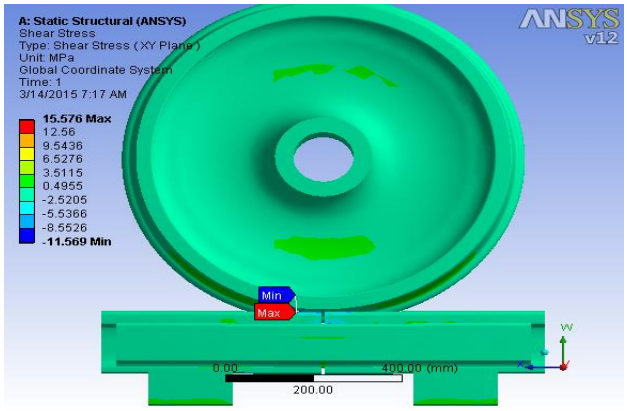

Figure 4.14: shear stress when M27 bolt is used.

And the shear stress is shown in the figure 4.10: the maximum shear stress is 15.576Mpa, and the minimum shear stress is -11.569Mpa.

C. Normal stress(bending stress)(MPa)

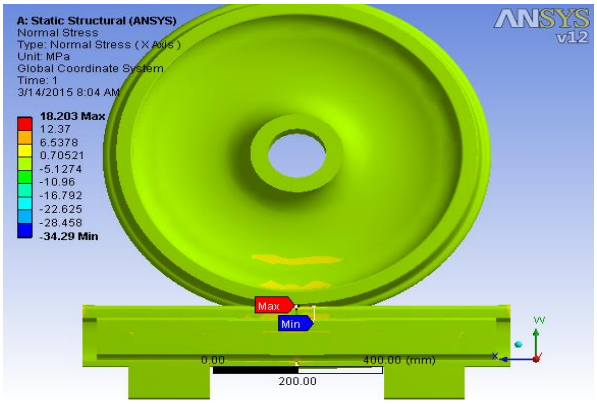

Figure 4.15: Normal stress when M27 bolt is used.

As shown in above figure 4.15: the maximum normal stress is 18.203MPa and the minimum Normal stress is -34.29MPa, when M27 bolt is used.

D. Safety factor

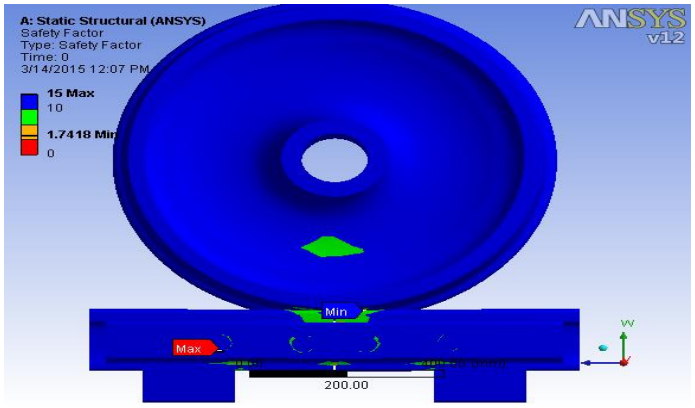

Figure 4.16: safety factor when M27 bolt is used.

As shown in above figure 4.16: the maximum safety factor is 15 and the minimum safety factor is 1.7418, when M27 bolt is used.

E. Stress on the fishplate and bolt

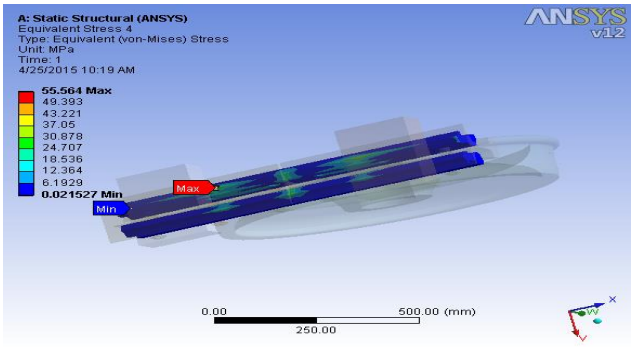

Figure: 4.17 equivalent stresses on the fish plate when M27 bolt is used.

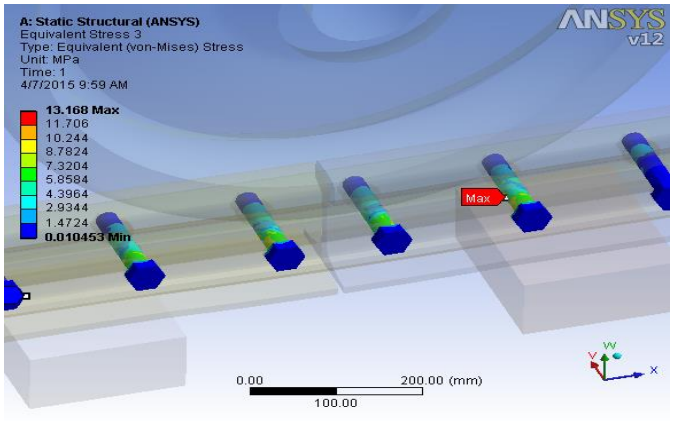

Figure: 4.18 equivalent stresses on the bolt when M27 bolt is used

ii. Stress on the bolts when different bolt materials are used

A. Stainless steel

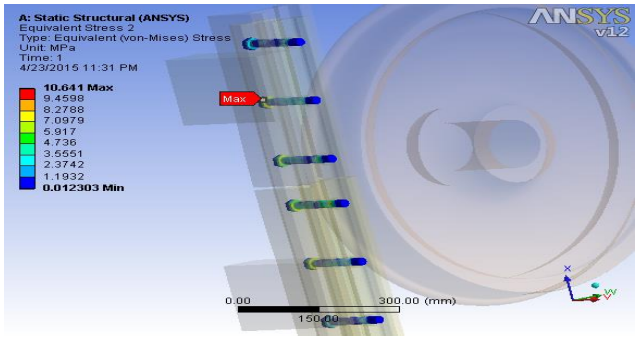

Figure: 4.19 equivalent stresses on the bolts when stainless steel is used.

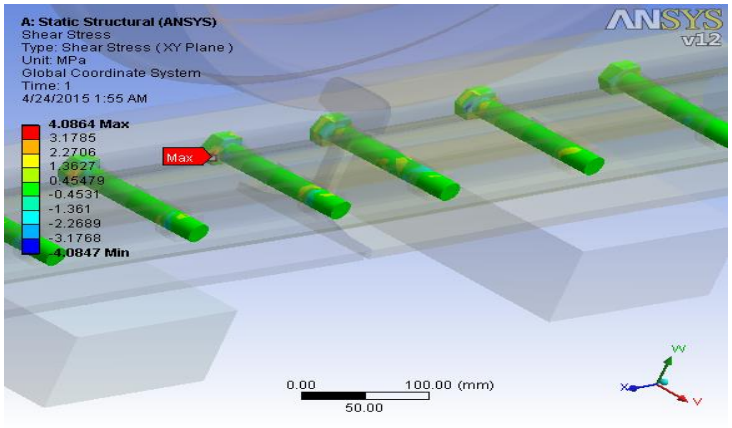

Figure: 4.20 shear stress on the bolts when stainless steel is used.

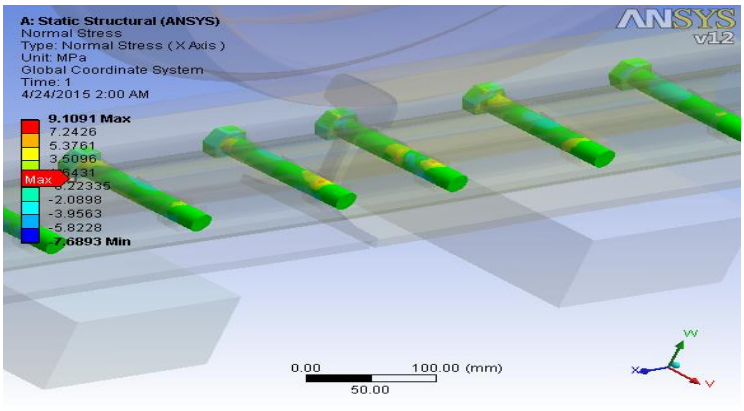

Figure: 4.21 Normal stresses on the bolts when stainless steel is used.

B. Low carbon steel (AISI 1018)

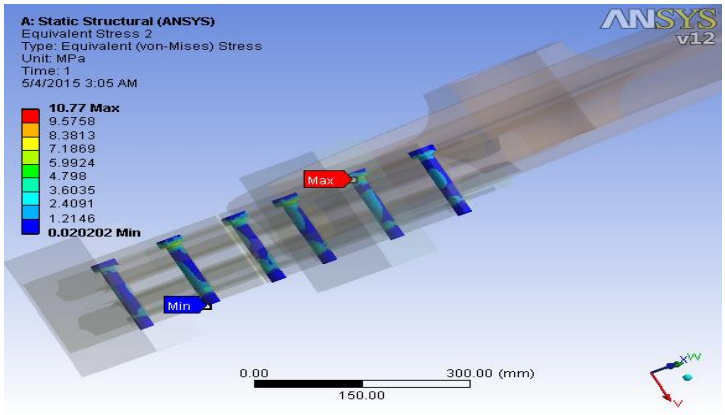

Figure: 4.22 equivalent stresses on the bolts when low carbon steel is used.

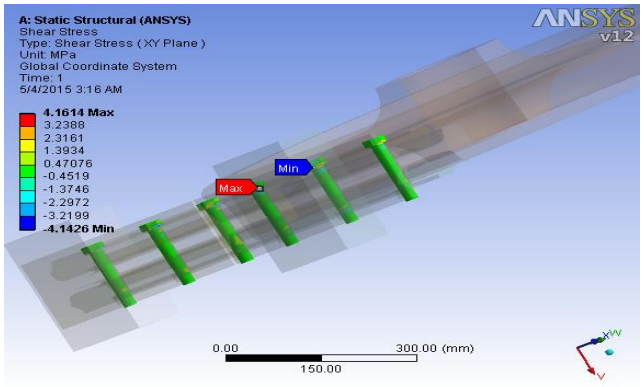

Figure: 4.23 shear stresses on the bolts when low carbon steel is used.

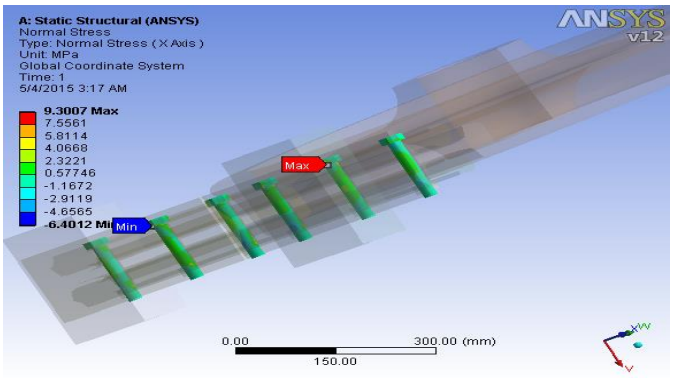

Figure: 4.24 Normal stresses on the bolts when low carbon steel is used.

C. Medium carbon steel (AISI 1035)

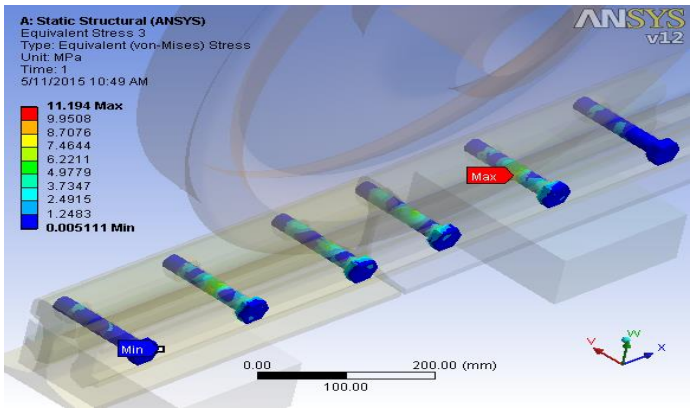

Figure: 4.25 equivalent stresses on the bolt when medium carbon steel is used.

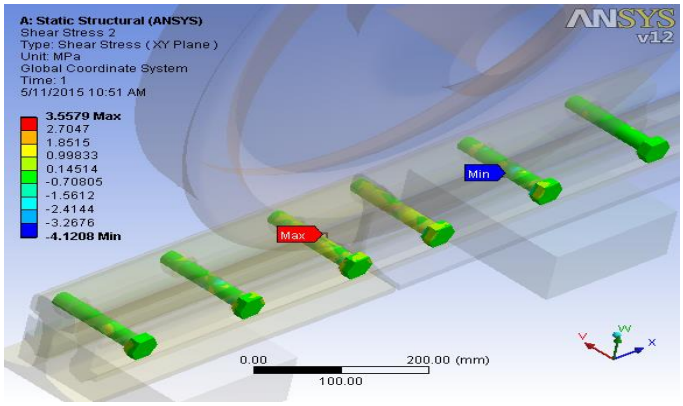

Figure: 4.26 shear stresses on the bolt when medium carbon steel is used.

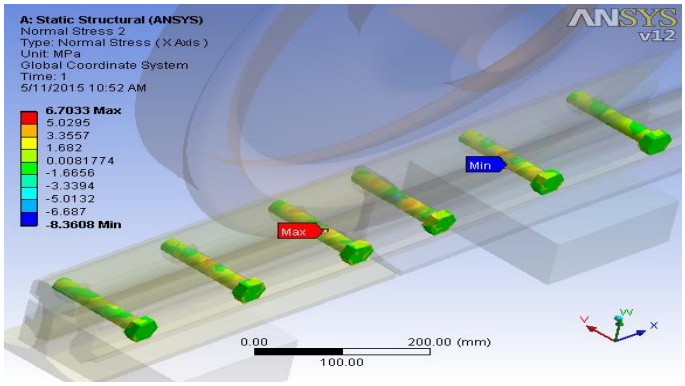

Figure: 4.27 Normal stresses on the bolt when medium carbon steel is used.

D. Alloy steel (AISI 4140)

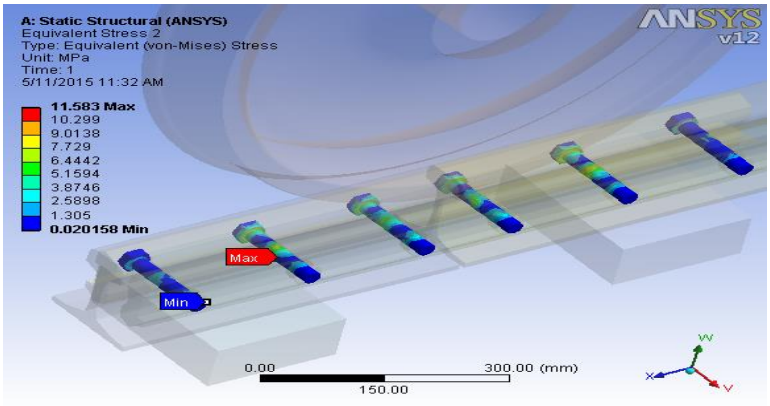

Figure: 4.28 equivalent stresses on the bolt when alloy steel is used.

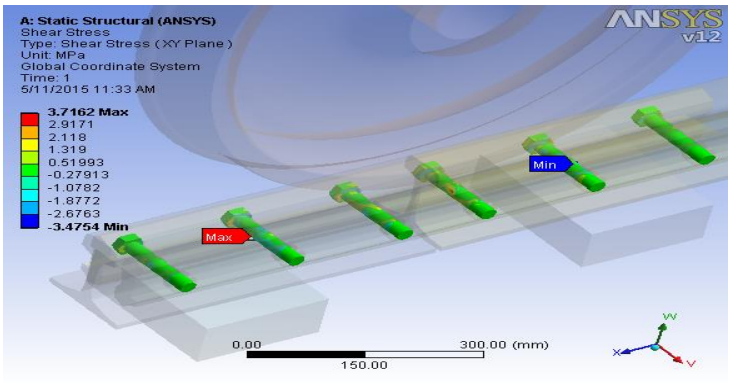

Figure: 4.29 Shear stresses when alloy steel is used.

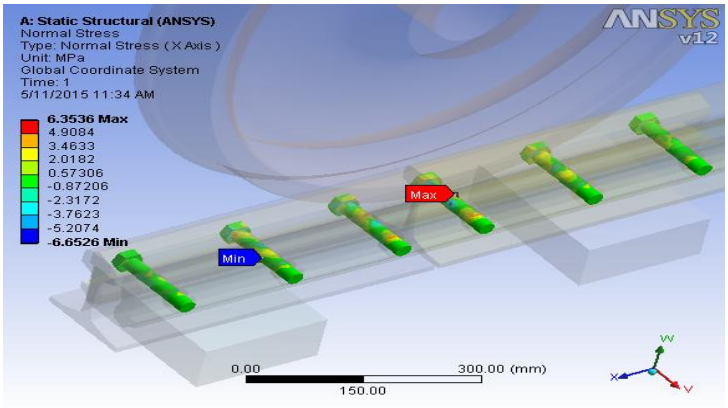

Figure: 4.30 Normal stresses when alloy steel is used.

4.2. Discussion

This section of the paper specifies the result obtained from the ANSYS software based on hertz contact theory. The above result shows different stress types and failure criteria due to vertical applied load at the rail joint. There are three different bolt geometries and bolt material compared each other like this.

From the ANSYS results shown in the above the stress in the joint is a little bit less in the joints with M22 bolts. The table 4.1 shows the difference of stress in the three bolt geometry.

Table 4.1: stresses in the three bolt geometry.

Stress		M22 bolt	M24 bolt	M27 bolt
Equivalent stress	Max.	59.482Mpa	57.939Mpa	55.564Mpa
	Min.	0.019436pa	0.005111pa	0.001043pa
Shear stress	Max.	18.273Mpa	16.238Mpa	15.576Mpa
	Min.	-17.549Mpa	-15.426Mpa	-11.569Mpa
Normal stress	Max.	19.384Mpa	19.585Mpa	18.203Mpa
	Min.	-39.861Mpa	-47.595Mpa	-34.29Mpa

Table 4.2: stresses in the bolt when different material is used.

Stress		Stainless steel	Low carbon steel	Medium carbon steel	Alloy steel
Equivalent stress	Max.	10.641Mpa	10.77Mpa	11.194Mpa	11.583Mpa
	Min.	0.0123Mpa	0.0202Mpa	0.0051Mpa	0.02016Mpa
Shear stress	Max.	4.0864Mpa	4.1614Mpa	3.558Mpa	3.7162Mpa
	Min.	-4.0847Mpa	-4.1426Mpa	-4.1208Mpa	-3.4754Mpa
Normal stress	Max.	9.11Mpa	9.301Mpa	6.7033Mpa	6.6526Mpa
	Min.	-7.6893Mpa	-6.4012Mpa	-8.361Mpa	-6.6526Mpa

The above result are included both rail joint and wheel for the reason of the analysis performed using the contact mechanism. This paper mainly focuses on joint part of rail for that matter it ignores the wheel result. As shown from ANSYS result the value of the stress is varying for the three types of bolts. In the M22 bolt as shown in the figure 4.1, figure 4.2, and figure 4.3 the maximum von mises, shear, and normal stress are 59.482MPa, 18.273MPa and 19.384Mpa. In the M24 bolt as shown in the figures 4.5, 4.6, and 4.7 the maximum von mises, and shear stresses are 57.939MPa, 16.238MPa, and 19.585Mpa. In the M27 bolt as shown in the figures 4.9, 4.10, and 4.11 the maximum von mises and shear, normal stresses are 55.564MPa, 15.576MPa, and 18.203Mpa all are around the bottom of the plate and nearest to the end head of the rail.

Stresses in bolts is shown above in the four different materials when stainless material is used as shown in the figures 4.19, 4.20, and 4.21 the maximum von misis , shear, and normal stress are 10.64Mpa, 4.0864Mpa, and 9.11Mpa. When low carbon steel material is used as shown in the figures 4.22, 4.23, and 4.24 the maximum von misis, shear, and normal stress are 10.77Mpa, 4.1614Mpa, and 9.30Mpa. When medium carbon steel material is used as shown in the figures 4.25, 4.26, and 4.27 the maximum von misis, shear, and normal stress are 11.194Mpa,

3.558Mpa, 6.703Mpa. When medium carbon steel material is used as shown in the figures 4.28, 4.29, and 4.30 the maximum von misis, shear, and normal stress are 11.583Mpa, 3.716Mpa, 6.526Mpa.

Chapter Five

5. Conclusion, recommendation and future works

5.1. Conclusion

A three-dimensional finite element model is used to analysis the bolt geometry and bolt material at rail joint section of track. The finite element program ANSYS is used to model the contact analysis. This ANSYS is used to simulate the loading and boundary conditions of the rail and wheel contact for a stress analysis. The effects of bolt geometry bolt material at rail joint are investigated. The results from the present investigation are indicates that the bolt geometry and bolt material have an effect on the equivalent and shear stresses.

5.2. Recommendations

While this thesis focused on the static loading of the rail joint, very little research has been performed using finite element analysis to model the dynamic loading of the joint. Impact loads can be significantly higher than static loads, especially when combined with larger displacements. From this research it was determined that by increasing the bolt diameter, the maximum stress of the joint was significantly decreased and when the bolt material is changed the stress also changed a little bit. The geometry of the bolt has seen to have an effect on stress of rail and joint it is better to use the best geometry and bolt material. The bottom of the plate, and the rail head are in high stress these parts should have strengthen to decrease fatigue and wear rate.

5.3. Future works

In this thesis work effects of bolt geometry and bolt material is observed on the stress of rail joint by finite element method using ANSYS software. Experimental study on the bolt geometry is also necessary to identify the stress more. The following points may be studied further in the rail joint analysis.

- Identifying the stress in the joint dynamically.
- Identifying crack initiation at the bolts.
- Effect of wear in rail joint using software's.
- Experimental measurement of fatigue and wear cracks in rail joint

References

[1]-Indraratna, B. and Wadud, S. (2005). Mechanics of Ballasted Rail Tracks: A Geotechnical Prospective. Taylor & Francis, London, UK.

[2]-Burton, P. (1975). "A Review of Rail Wheel Contact Stress Problems." Proceedings of Symposium on Railroad Track Mechanics.Pergamon Press, Englewood Cliffs, NJ.

[3]- Chandrupatia, Tirupati R. & Ashok D. Belegundu, Introduction To the finite Elements in Engineering, Prentice hall of India Pvt. Ltd., New Delhi.Int. J. Mech. Sci, ASME. 1999;41;1253-72.

[4]-Wen Z. Jin X. Zhang W. Contact-impact stress analysis of rail joint region using the dynamic finite element method, Wear, 2005;258;1301-09.

[5]-Chen, Y. C. and Kuang, J. H. (2002). "Contact Stress Variations near the Insulated Rail Joints." Proceedings of the Institution of Mechanical Engineers, Part F, Journal of Rail and Rapid Transit, Vol. 216, No. 4, pp. 265-273.

[6]-N. Zong, D. Wexler, & M. Dhanasekar Structural and Material Characterization of Insulated Rail Joints Electronic Journal of Structural Engineering 13(1) 2013 University of Technology, Brisbane, Australia

[7]-Cai, Wu; Wen, Z; X. ; Zhai, W., Dynamic stress analysis of rail joint with height difference defect using finite element method, Engineering Failure Analysis 14, pp 1488-1499, 2007.

[8]-Davis, D. D., Collard, D., and Guillen, D. G. (2004). "Bonded Insulated Joint Performancein Mainline Track." Technology Digest, May, 2004.

[9]- Chen, Y. C. (2003). "The Effect of Proximity of a Rail End in Elastic-Plastic Contact Between a Wheel and a Rail." Proceedings of the Institution of Mechanical Engineers, Part F, Journal of Rail and Rapid Transit, Vol. 217, pp. 189-201.

[10]-Kerr, A. D. (2003). Fundamentals of Railway Track Engineering. Simmons-Boardman Books, Omaha, NE.

[11]-Kerr AD, Cox JE. Analysis and test of bonded rail joints subjected to vertical wheel loads,

[12]-Profillidis, V. A. (2000). Railway Engineering. Ashgate, Burlington, VT.

[13]-Nannan Zong and Manicka Dhanasekar, 2012: Analysis of Rail Ends Under Wheel Contact Loading, International Journal of Mechanical and Aerospace Engineering 6, 452-460.

[14]-Muhammad Akhtar , David Davis , Luis Maal Jeff Gordon and David Jeong, 2010: Effects Of Track Parameters on Rail Joint Bar Stresses and Crack Growth, AREMA Annual Conference and Exposition Orlando, Florida

[15]-Sunil Patel, Veerendra Kumar and Raji Nareliya,Jan2013:Fatigue Analysis Of Rail Joint Using Finite Element Method, vol2, ISSN2319-1163

[16]-Nirmal Kumar Mandal and Brendan Peach, 2010: An Engineering Analysis of Insulated Rail Joints, A General Perspective" International journal of engineering science and technology, vol2,2(8),3964-3988.

[17]-Nicolae Faur , Ion Goia , LaurenŃiu Culea, Anghel Cernescu and Assistent Radu Negru, Nov 2007:Stress-Strain Analysis For the Wheel-Rail Track Assembly at Urban Passenger Transport,5th Int. Conference Structural Integrity of Welded Structures (ISCS2007), Timisora, Romania, 20-21

[18]-Hiroo KATAOKA, Noritsugi ABE and Osamu Wakatsuk: Evaluation of Service Life of Jointed Rails, Track Structure & Component Group, Railway Technical Research Institute, Japan

[19]-Anne K. Himebaugh, November 28, 2006: Finite Element Analysis of Insulated Railroad Joints, Master of Science In Civil Engineering,1-75

[20]-Daniel Peltier, Christopher P. L. Barkan, Engineering Steven Downing and Darrell Socie: Measuring Degradation of Bonded Insulated Rail Joints, University of Illinois at Urbana-Champaign Urbana, IL 61801

[21]- Mohammad Hossein Abolbashari, Reza Ahrari A Simplified Finite Element Model for the Insulated Rail Joint Bar Stress Analysis 17th.Annual (International) Conference on Mechanical Engineering-ISME2009 May, 2009, University of Tehran, Iran

[22]-Zachary I. Charlton, April 10, 2007: Innovative Design Concepts for Insulated Joints, Master of Science ,Blacksburg, Virginia

[23]-Brandon Talamini, David and Y. Jeong, March 13-16,2007:Estimation of the Fatigue Life of Railroad Joint Bars, 2007 ASME/IEEE Joint Rail Conference & Internal Combustion Engine Spring Technical Conference,1-10

[24]-Prachi Katheriya, Veerendra Kumar an investigation of effects of axle load and train speed at rail joint using finite element method International Journal of Research in Engineering and Technology

[25]-Jiangtao Song and Randy J Gu, 01- 05 June 2008: A Finite Element Based Methodology for Inverse Problem of Determining Contact Forces Using Measured Displacements, International Conference on Engineering Optimization.